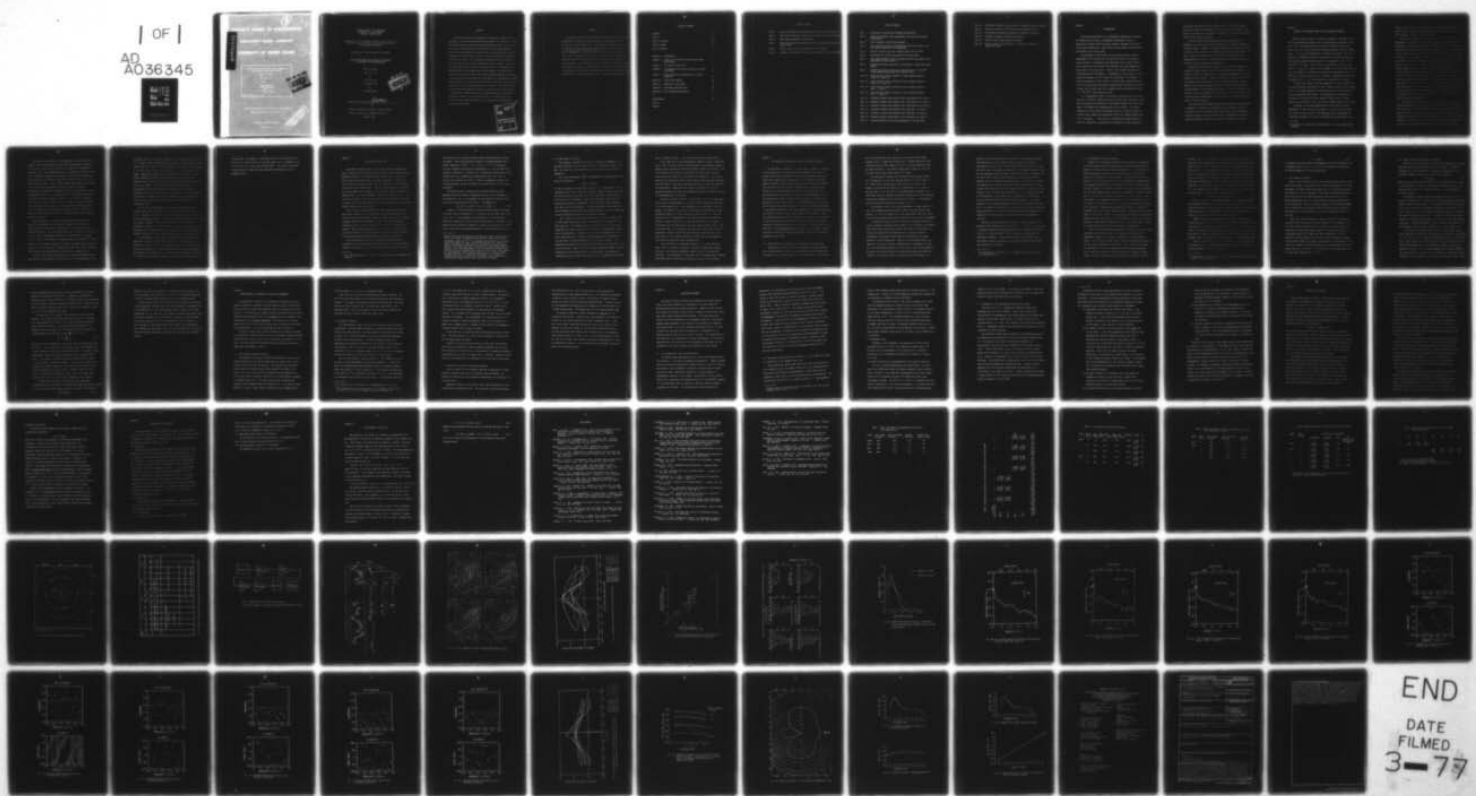


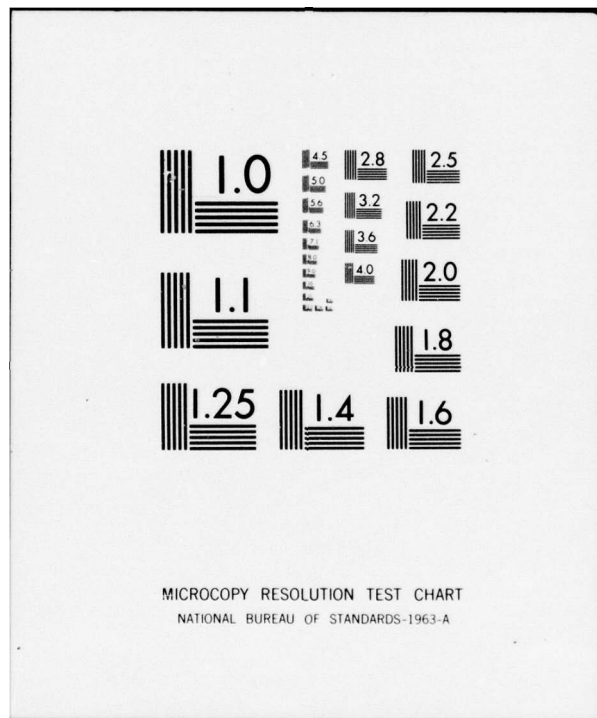
AD-A036 345

RHODE ISLAND UNIV KINGSTON GRADUATE SCHOOL OF OCEANO--ETC F/G 4/2
OCEANIC WIND SPEED AND WIND STRESS ESTIMATION FROM AMBIENT NOIS--ETC(U)
FEB 77 P SHAW, D R WATTS, H T ROSSBY N00014-76-C-0226
UNCLASSIFIED URI/GSO-REF-77-2 NSF-MODE-CONTRIB-87 NL

| OF |
AD
A036345



END
DATE
FILED
3-77



GRADUATE SCHOOL OF OCEANOGRAPHY
UNIVERSITY OF RHODE ISLAND
KINGSTON, RHODE ISLAND

Reproduction of the material contained in this report in
whole or in part is permitted for any purpose of the
United States Government

Distribution of this document is unlimited

Oceanic Wind Speed and Wind Stress Estimation from Ambient Noise Measurements

Technical Report

Ref. No. 77-2

by

Ping-Tung Shaw

D. Randolph Watts

and

H. Thomas Rossby

Approved for Distribution

Partially Sponsored by Office of Naval Research

Report under Contract N00014-76-C-0226

February 1977

7

ABSTRACT

From ship records of wind speed and 5 kHz acoustic ambient noise measured on ocean bottom instruments during MODE-I, we find that the noise records may be used to monitor wind speed and wind stress over the ocean. Time series of wind speeds can be produced from noise measurements via the linear relationship we find between the noise spectrum level and the logarithm of the wind speed. Errors in this conversion are estimated to be less than 5 knots. By independently determining the wind direction, the wind stress has also been estimated and vector-averaged. In this way the mean wind stress is neither fair-weather biased nor systematically underestimated from the mean wind velocity squared. The monthly mean stress from our data is higher than values computed from mean wind speeds or from probability distributions of wind speeds in climatological records. Power spectra of our wind speed records decrease smoothly with increasing frequency ($f^{-1.5}$) for periods between 2 to 50 hours. The noise pressure records exhibited significant coherence between pairs of localities 100 to 200 km apart during the spring, as organized weather fronts passed through the region. Cross-correlation time lags between sites were consistent with a mean propagation of the atmospheric disturbances of 30 km/hr southeastward.

ACCESSION FOR	White Section <input checked="" type="checkbox"/>
RWS	Buff Section <input type="checkbox"/>
B&G	<input type="checkbox"/>
UNARMED	<input type="checkbox"/>
JUSTIFICATION
BY	
DISTRIBUTION/AVAILABILITY CODES	
Dist.	AVAIL. AND/OR SPECIAL
A	

PREFACE

The report in this form was submitted by Ping-Tung Shaw as partial fulfillment of a Masters of Science degreee in Oceanography at the University of Rhode Island, 1977. The data were collected as part of the Mid-Ocean Dynamics Experiment (MODE), primarily aboard cruises of the R/V RESEARCHER in the western North Atlantic Ocean during March-July, 1973. The ambient noise records were obtained by Inverted Echo Sounders financed by the National Science Foundation grant GX30416 to Yale University. Ping-Tung Shaw was the recipient of a graduate fellowship from the University of Rhode Island. The analyses reported herein were supported by the Office of Naval Research under contract N00014-76-C-0226 to the University of Rhode Island. This is Mode contribution #87.

TABLE OF CONTENTS

Abstract	1
Preface	ii
Table of Contents	iii
List of Tables	iv
List of Figures	v
Chapter 1 Introduction	1
Chapter 2 Review of the ambient noise and wind speed relationship	3
Chapter 3 The noise and wind data	8
Chapter 4 The empirical wind-noise relation and stress estimation	12
Chapter 5 Power spectra and coherences of rms noise pressures	21
Chapter 6 Application remarks	25
Chapter 7 Summary and conclusions	31
Appendix A Instrument specifications	34
Appendix B The instrument calibration	36
Bibliography	38
Tables	
Figures	

LIST OF TABLES

Table 1 Mean wind speeds and standard deviations from ship observations

Table 2 Peak cross-correlation coefficients between noise and wind speed

Table 3 Least-square regression coefficients

Table 4 Mean wind speeds and standard deviations calculated from ambient noise levels

Table 5 Monthly mean wind stress derived from noise series

Table 6 Maximum cross-correlation coefficients between noise level series

✓

LIST OF FIGURES

Fig. 1 Positions of Inverted Echo Sounders during MODE-I

Fig. 2 Duration of ambient noise measurements and wind speed records during MODE-I

Fig. 3 Block diagram of IES noise measurement

Fig. 4 Noise spectrum levels at three IES sites and wind speed of the same period observed by R/V Researcher

Fig. 5 Six-hour synoptic sea level pressure maps, March 27, 1973

Fig. 6 Correlation of various noise series with wind speed

Fig. 7 Wind speed observed versus wind speed derived from ambient noise measurement of IES at site A

Fig. 8 Probability density functions of wind speed in 3-knot wind speed groups

Fig. 9 Probability density functions of wind stress in 0.5 dyne/cm^2 groups computed from noise level series C and G

Fig. 10a Power spectral density function of noise pressure series A (March 25 - April 11)

Fig. 10b Power spectral density function of noise pressure series C (March 25 - April 11)

Fig. 10c Power spectral density function of noise pressure series G (May 7 - June 18)

Fig. 10d Power spectral density function of noise pressure series H (May 7 - June 18)

Fig. 11a Coherence between noise series A and B from March 25 to April 11

Fig. 11b Coherence between noise series A and C from March 25 to April 11

Fig. 11c Coherence between noise series B and C from March 25 to April 11

Fig. 11d Coherence between noise series E and G from May 7 to June 18

Fig. 11e Coherence between noise series E and H from May 7 to June 18

Fig. 11f Coherence between noise series G and H from May 7 to June 18

Fig. 12 Cross-correlation of rms noise pressures of two IES sites

Fig. 13 Theoretical spectra of rain noise for different rates of rainfall

Fig. A1 Directivity pattern of IES receiving hydrophone at 5 kHz

Fig. A2 IES transducer receiving response in horizontal direction

Fig. A3 Frequency response of broad band amplifier

Fig. B1 Ambient noise system frequency response

Fig. B2 Input voltage of log detector as a function of output of frequency counter

Chapter 1

INTRODUCTION

Wind stress measurement is of considerable importance in studying the response of the ocean to atmospheric disturbances, such as: generation of surface waves and drift currents, deepening of the wind-mixed layer (Pollard, 1973), eddy motion (Phillips, 1966), and wind-driven circulation of the entire ocean.

The knowledge of wind stress over the ocean requires a detailed measurement of the structure of the wind field close to the surface. Several methods of measurement were described by Roll (1965); however those methods are not practical for continuous long term measurement of wind stress in the open ocean. Instead, most estimates are made from climatological wind information. Unfortunately, errors occur due to the quadratic dependence of wind stress upon wind speed. For example, in their investigation of wind stress in the open ocean, Deman and Miyake (1973) found that mean wind stress, computed from individual wind speed records, is 50% higher than that computed directly from mean wind speed (i.e. $\overline{v^2} \approx 1.5 \overline{v^2}$ in this particular case).

In a comprehensive study of the global distribution of wind stress, Hellerman (1965, 1967) compiled monthly and annual mean wind stress tables from the frequency distribution of wind speeds instead of the mean wind speed. This method only eliminated part of the errors. In a recent computation of wind stress from weather reports of ships in the North Atlantic Ocean, Bunker and Worthington (1976) got a higher average than that of Hellerman. They noted the difference had arisen from their method of computation, specifically by computing the vector average of

wind stress from individual wind speed records. Even so, the results obtained by using their method may not be correct, because ships avoid areas of high wind and the quadratic dependence of wind stress upon wind speed further biases the results.

The above mentioned shortcomings have no simple resolution, especially in view of the fact that two-thirds of the earth's surface is covered by water. However, it has been known for some time that a high correlation exists between wind speed and the acoustic noise level in the ocean. This thesis explores the hypothesis that the ambient noise measurements can be used for monitoring unbiased surface wind speed and stress in any open ocean area (Rossby, 1973).

Correlation calculations are used in this study to interpret the connection between ambient noise levels and observed wind speeds. It is found that their relationship can be accurately represented by a least-squares best-fit equation. Series of surface wind speeds are converted from ambient noise measurements for wind speeds higher than 5 knots. Series of wind stress computed from these individual wind speeds are vector-averaged to get the mean wind stress. The wind directions were supplied by the R/V Researcher, but information from other sources, such as the satellite observations of cloud motion or the surface pressure charts, can also be used.

The close relation between wind speed and ambient noise also makes it possible to describe the correlation of wind speeds at pairs of localities from the coherence between their ambient noise pressures. In this way, several instruments can be used to investigate, in the wave number and frequency domain, the spectrum of winds over the ocean.

Chapter 2

REVIEW OF THE AMBIENT NOISE AND WIND SPEED RELATIONSHIP

Acoustic ambient noise in the ocean is defined as "that part of the total noise background observed with a non-directional hydrophone, which is not due to the hydrophone and its manner of mounting called 'self noise', nor due to some identifiable localized sources of noise" (Urick, 1975). It is the noise generated by the ocean environment. The unit of intensity of underwater sound is the intensity of a plane wave having a rms (root mean square) pressure equal to 1 micropascal ($1 \mu\text{Pa} = 10^{-5}$ dyne/cm² or $10^{-5} \mu\text{bar}$). Noise level is then defined as $N \text{ dB re } 1 \mu\text{Pa}$ with $N = 10 \log \frac{I_N}{I_0}$, where I_N is the energy of the noise sound wave and I_0 is the energy of a reference sound wave with rms pressure $1 \mu\text{Pa}$.^{*} In practice, the noise spectrum level (in dB/Hz) is specified as the amount of energy in dB units one would measure in a pass band of 1 Hz wide.

In this study, ambient noise was measured at a depth of 5000 m and the noise frequency monitored was 5 kHz. Ambient noise at this frequency falls in the range described by Knudsen curves which are wind speed and sea state dependent (Wenz, 1962). Two advantages for this choice of frequency can be seen from Wenz's spectra: surface wind is the most dominant noise source at 5 kHz, and distant shipping noise is not present.

According to the noise spectra given by Wenz (1962), the wind dependence of noise levels in the range 1 to 10 kHz are very similar. The results of many studies of wind generated noise, though made for frequencies between 1 and 3 kHz, can therefore be extrapolated to the

* The energy of a sound wave is proportional to the mean square sound pressure.

study of 5 kHz noise. In later discussions, "wind dependent noise" is used to refer to the noise at frequencies between 1 and 10 kHz, and the exact frequency range will not be mentioned.

Although the processes of noise generation are still not clear, the sea surface is considered to be the major source in Knudsen's spectra (Wenz,1962). Breaking white caps and the collapse of air bubbles near the surface may be important at high wind speeds, but the wind dependence of noise level occurs far before waves break for wind speeds as low as 5 knots (1 knot = 0.52 m/sec). Therefore, it is likely that other processes are present. Marsh (1965) successfully expressed Knudsen curves in both deep and shallow water by giving a quantitative formula based on the Longuet-Higgins' theory of surface waves (Longuet-Higgins,1950). Kuo (1968) proposed another physical model by a hypothesis that ambient noise in the deep ocean is caused by randomly distributed high frequency capillary patches at the sea surface. His model agrees well with actual observations. So far this is the most advanced model for the process of noise generation by wind. According to these models, ambient noise level can also be related to the wave height, but the observations show that the dependence of noise level on wave height is much less than wind speed (Frish,1966; Perrone,1969).

Other sources which may affect the 5 kHz ambient noise level are local precipitation and heavy shipping noise (Wenz,1962). These sources only have local and transient effects, and have spectra different from those described by Knudsen. The effects of bottom composition can be neglected by using a hydrophone with high sensitivity only in the upward direction. Biological noise sources, such as shrimps and croakers, may contribute to 5 kHz noise, but they rarely live in depths of 5000 m.

The theory of Kuo (1968) and the observations of Wenz (1962) and Perrone (1970) all agree with the idea that the generation of noise by wind is only a local effect; however, it is difficult to estimate how localized it is. The estimates involve the consideration of many factors, such as spherical spreading of sound waves, the absorption coefficient, sound refraction in the water column, and reflection losses both at the bottom and the surface. Most of these factors depend upon the conditions at the site of noise measurement and are not easy to determine.

Nevertheless, an estimate is proposed as follows: The directivity study of deep-sea noise at 1414 Hz showed that the -3 dB points are nearly at 45° from the vertical (Axelrod et al, 1965). At 5 kHz the attenuation coefficient for sound is higher (about 0.3 dB/km) and one would expect the contributing noise sources to be more localized, probably within a 5 to 10 km range for an instrument at a depth of 5000 m. However, the problem of predicting the directivity is complicated by the ray bending effects in the ocean.

Cross-correlation of noise with wind speed has been used as a quantitative demonstration of the wind dependence of ambient noise. High noise-wind correlation has been found for 1 kHz deep water noise (Perrone, 1969; 1970). For wind speeds lower than 7.5 knots, the correlation is low. This low correlation was due to the contribution of shipping noise at 1 kHz. The influence of shipping noise is much smaller at 5 kHz, because of the increased absorption of distant shipping noise by sea water relative to local wind noise at frequencies higher than 1 kHz. Furthermore ships generate less high frequency noise than low frequency noise.

The close relationship established by the cross-correlation study of wind speed and wind-generated noise was first put into mathematical form

by Piggott (1964) by using data obtained in very shallow water (about 40 m). He used a simple linear equation to express the noise spectrum level (NSL) in dB as a function of the logarithm of wind speed (V) in knots: $NSL = 20 M \log (V/V_0)$, where M is the slope and V_0 is some reference wind speed. Based upon Perrone's data (Perrone, 1969; 1970), Crouch and Burt (1972) extended this linear relationship empirically to deep water conditions (about 5000 m) by including a non-wind dependent term into the total noise energy. Fig. 1 in their paper clearly shows that the proportionality of noise level with the logarithm of wind speed for frequencies between 1414 and 2816 Hz is very good. The non-wind dependent portion is important only when wind speed is lower than 10 knots. Their results coincide with the 7.5 knot limit found in Perrone's correlation study.

For the wind speeds higher than 10 knots and noise frequencies between 1 and 3 kHz, Crouch and Burt (1972) found the slope M to be 1.00 ± 0.04 . Piggott's study (1964) in shallow water had a slope 20% higher in the same frequency range. Although the slopes for deep and shallow water are slightly different, both authors concluded that the slopes are essentially constant. As mentioned above, in spite of the fact that no references give information about the relationship between wind speed and ambient noise level at 5 kHz, similar characteristics can be expected.

The uncertainty of noise levels under different wind conditions is found both in the field data (Perrone, 1969) and in the empirical relationship of Crouch and Burt. This uncertainty may result from the variation of air stability near the sea surface; however, no such dependence was studied in the literature. Ambient noise levels grouped in intervals of 5 knots of wind speed show higher uncertainty for weak winds than for

strong winds. For example, the standard deviation of the noise level at 2816 Hz is 0.7 dB in the 47.5 to 52.5 knot group, but it increases to 2.5 dB in the 2.5 to 7.5 knot group (Perrone, 1969). The linear relationship is more useful for high wind speed conditions, particularly for low frequency sound.

Chapter 3

THE NOISE AND WIND DATA

The ambient acoustic noise at 5 kHz was an auxillary measurement made by seven Inverted Echo Sounders (IES) during the Mid-Ocean Dynamics Experiment (MODE-I) in the western North Atlantic Ocean. The IES is a bottom mounted instrument which is primarily designed to measure the travel time of an acoustic signal from the ocean bottom to the surface and back (Watts and Rossby, 1976). However, during MODE each instrument was also equipped with a separate 5 kHz transducer which monitored the ambient noise. The seven instrument locations are shown in Fig. 1. Two twenty day records and one forty-five day record were obtained in March and April, 1973, and there were three fifty day records and one forty day record in May and June, 1973 (Fig.2).

Fig. 3 shows a block diagram of the noise measurement circuitry. Noise signals received by the hydrophone were amplified and filtered. They were then passed through a logarithmic peak detector and a voltage-frequency converter (V-F converter). Every 4 minutes the variable frequency output of the V-F converter was counted for a period of 24 seconds*. These counts are proportional to the acoustic noise levels. They were recorded on a digital cassette recorder for further analysis. The detailed instrument specifications are listed in Appendix A.

One design-weakness with the measurement technique should be recognized: the sampling frequency associated with the 4 minute sampling interval (1/4 minutes) is ten times lower than the bandwidth (1/24 sec)

* This noise measurement and the echo sounding were done in separate time intervals.

resulting from the 24 second averaging time (counting period) for each instrument. This could potentially result in aliasing problems with a Nyquist frequency $(8 \text{ min})^{-1}$. Later averaging of the noise pressures will only increase the statistical significance but will not affect the aliasing. Empirically, aliasing is not a significant problem here, since aliasing would only degrade the correlations studied below, and the observed correlations were high.* In order to completely eliminate the aliasing problems, we have to sample at the same interval as the averaging period.

The equation used in converting the recorded counts to noise spectrum levels was derived by measuring the gain of the instrument in the laboratory. Eq. (3.1) expresses the relationship between the count (C) and the noise spectrum level (NSL). (see Appendix B)

$$\text{NSL (dB re } 1 \mu\text{Pa/Hz)} = 21.5 + 0.00561 \times C \quad (3.1)$$

There is a $\pm 20\%$ uncertainty in the system gain from one instrument to another, which corresponds to a ± 2 dB error in the offset term (21.5) of Eq. (3.1). This uncertainty can be reduced by calibrating each instrument respectively to get the converting equation. The error in the proportionality constant is expected to affect the noise level by 0.5 dB, which is less than the standard deviation of deep sea noise levels even

* Oceanic wind speed spectra given by Byshev and Ivanov (1969) show that most of the energy is associated with periods longer than one day, decreasing roughly as $f^{-5/3}$ to a minimum around periods of 8 minutes; beyond that there is a small spectral bump centered at a period of 1 minute, presumably associated with an increase in wind-gust energy density. The Byshev and Ivanov spectra are for wind speed measured at one point (i.e. ship measurements). The corresponding ambient noise spectra arise from sources within roughly a 10 km circle, and because of this averaging, there might not be any bump at 1 minute period. Nevertheless, this is a necessary measurement in the future, to eliminate aliasing or confirm that the ambient noise spectra fall to insignificant energy density beyond some known frequency.

at a wind speed of 50 knots.

The frequency response of the system is primarily determined by the transducer response, and is a band centered at 5 kHz with a width of 1.4 kHz. The details for the determination of the band width are listed in Appendix B.

The noise rms pressure ($\sqrt{\langle p^2 \rangle}$) transformed from noise spectrum level (NSL) by the equation

$$\sqrt{\langle p^2 \rangle} = 10^{\text{NSL}/20},$$

is used in computing the mean noise pressure of 15 measurements. A few anomalously high counts, which are apparently caused by system malfunction and which constitute less than 0.1% of the total data, were excluded in the calculation of the means. Hourly noise spectrum levels were then computed from those mean pressures. These two hourly series obtained were used in the later analyses. They were examined at times when the ship R/V Researcher was known to be working within 10 km of the IES's and no noise contamination from the ship could be detected.

Fig. 4 shows the three noise level series A, B and C together with the wind speed observations of the R/V Researcher, all relative to the same time axis. The primary source of information used in this study, regarding the wind in the MODE area, consists of meteorological observations from Researcher. Although the wind records themselves are very good, these data are of limited usefulness because of the movement of the ship about the entire MODE area (a 200 km radius circle). The observed wind speeds may not be exactly the same as the ones within 10 km of the IES sites. However, this is the best information available which describes the local weather conditions during MODE. The mean and the standard deviation of wind speeds recorded by R/V Researcher during each

month is listed in Table 1. The cruise durations are shown in Fig. 2.

In the first set of noise measurements (series A, B and C; March and April, 1973), the wind field was characterized by the repeated passage of weather fronts through the MODE area advancing toward the southeast. Most of the energy of the winds was associated with these fronts, which by their nature vary rapidly in the direction of propagation. The surface winds and the associated ambient noise generated from them were organized along the fronts, were highly localized across the fronts, and propagated with the fronts. Therefore, they arrive at different IES sites at a rather well defined lag time which depends upon their orientation relative to the propagation of the fronts.

During two periods, March 25 to 28 and April 6 to 10, the wind speed data overlap the measurements of all three noise series and the patterns of the noise series have a close resemblance to the pattern of the wind speeds. For example, the buildup to high winds on March 26 has the corresponding shape in all noise series (see arrows in Fig. 4). Both the weather log of R/V Researcher and the surface pressure charts show the passage of squall lines (Fig. 5) with gust wind from 30 to 45 knots. It is possible that the high noise levels were partly caused by rain. With our limited data, the contribution of rain to the total noise can not be determined. However, since heavy precipitation occurs only in a very small portion of the weather records, its effect may not be important in long term wind stress and speed investigations.

In the second set of experiments (series D, E, G and H; May and June, 1973), by contrast, virtually no fronts or storms moved through that area. The winds were generally lighter (Table 1) and less well organized. This description is consistent with the ambient noise observed during that period showing poor correlation from one site to another.

Chapter 4

THE EMPIRICAL WIND-NOISE RELATION AND STRESS ESTIMATION

The preliminary overview in the latter part of chapter 3, discussing the prevailing wind field during this experiment, will help to explain the following sequence of analyses and anticipate some of the results and limitations of this method. The existence of high wind speeds and weather fronts in March and April had a profound influence upon the data, both for individual ambient noise monitoring sites (fixed) and for ship observations (mobile) of surface winds. Our analysis procedures were chosen to deal with the inadequacies of the wind observations, which ideally should be directly over each IES. A description of our method follows. The cross-correlation of the wind and the noise time series was plotted. At the time-lag corresponding to the maximum correlation, the linear regression of wind and noise was calculated for each site that showed significant correlation. Those best regression coefficients were then used uniformly at all IES sites to scale the noise measurements into wind speed records for further statistical characterization of the wind speed and stress fields in the MODE area. Wind directions determined aboard ship were used. Comparisons will be drawn with historical information about the wind stress estimated in that area.

4.1 Cross-correlation between noise rms pressure and wind speed

When pairs of noise series and wind speed records were available for a certain period of time, their cross-correlation functions were calculated, with the mean values of each series removed. The correla-

tion coefficients were then normalized to have their values range between -1 and +1 (Bendat and Piersol, 1971). Maximum lag time in each correlation function was chosen to be 10% of the data length available for each calculation. The highest correlations occurred at time lags less than these chosen maximum lags in all cases.

The time span of series A and B overlaps the wind speed records of R/V Researcher for two short periods: March 22 to 28 and April 6 to 11. They can only provide usable data for 70 to 133 hours. For series C in April and all series of the second set (D, E, G and H of May and June), 378 to 480 hours of overlapping data are usable. For each noise series the maximum correlation coefficient and its associated time lag are summarized for various months in Table 2. The associated plots of correlation functions are shown in Fig. 6.

Two features in Fig. 6 are worth discussing: (1) April series A, B and C have higher maximum correlation coefficients than the May-June series. (2) Plots of series A and B show sharp peaks, while all others have slowly decreasing correlation functions as the lag time is increased.

A correlation function with low and slowly decreasing correlation could be caused by extraneous noise sources, or the absence of correlated local wind fields between each IES and ship sites, or the varying time lags due to movement of the observing ship. Shipping noise and instrumental "self-noise" could cause low correlation in the usual fashion at low wind conditions. However, this extraneous noise is not important in our study: distant shipping noise is negligible at 5 kHz due to the increased absorption of sound in the ocean, and the possible existence of ship noise caused by ships closely passing the IES's was expelled, as mentioned before, by reviewing the noise records. In

addition, no IES "self-noise" could be found. The spatially organized wind fields are, in fact, absent during the second set of noise measurements (May and June), but are present during the first set (March and April) when the weather was dominated by the repeated passage of weak but well-organized frontal systems through the MODE area. Therefore, in the latter case, there are good correlations along the fronts and at specific time lags between sites perpendicular to the fronts. Although high peaks exist at specific time lags between fixed observation sites, a mobile ship observation will mix together different time lags and thus broaden as well as reduce the correlation peak. By examining the track of R/V Researcher, it was found that the positions of the ship were fairly scattered during the 480 hour period of series C. The broad maximum of the correlation function of series C is consistent with this fact. The correlation functions of series C and all May-June series are seriously affected by the fact that the wind speeds were measured by a moving ship. Those series are not suitable for linear regression analysis.

Besides the cross-correlation functions, coherence between noise series and wind speeds were also calculated. Only series C in April has a coherence significantly different from zero at frequencies less than 0.25 C.P.H. (cycle per hour).* All the May and June series have no significant coherence. These results confirm the conclusion given by the cross-correlation functions, so no further discussion about noise-wind coherence is necessary.

* The data lengths of series A and B in March and April are too short for coherence study.

4.2 The empirical linear relationship

Series A and B in March and April as well as series C in March are the most suitable series for determining the wind-noise relationship, because of the high winds and better correlations. In this section the linear relationship between the noise spectrum level in dB and the logarithm of wind speed in knots proposed by Crouch and Burt (1972) is applied to the IES noise data and the R/V Researcher wind speed records. The regression coefficients are computed by the method of least-squares. The error caused by the separation between the sites of noise measurements and wind speed observations is partially eliminated by shifting the time scale by the time lag of maximum correlation, listed in Table 2. Mean wind speeds for the sampling periods are 13 to 21 knots (Table 3). In the report by Crouch and Burt (1972), the total noise energy is resolved into two parts, a constant non-wind dependent term and a linear wind dependent term. The non-wind dependent term is important only when wind speed is lower than 10 knots. Since the mean wind speeds of the sampling periods are quite high, and at a noise frequency of 5 kHz, the non-wind dependent noise should be unimportant even at wind speeds below 10 knots, the linear term is the only one which should be considered.

Table 3 lists least-squares regression coefficients, where the noise spectrum level (in dB re 1 μ Pa) is the dependent variable and the independent variable is 20 times the logarithm of the wind speed (in knots). It also lists the mean noise levels and the mean wind speeds of the data used in regression calculations. The F values of all series are significant, so all five regression coefficients are meaningful. Four of the five noise level-wind speed pairs have regression slopes around 1.01 with a 10% error and the intercepts vary within 2 dB from

the mean value. It is clear that a common linear relation exists in these four. The slopes agree with that extrapolated from the results of Crouch and Burt (1972).^{*} Series B in March deviates significantly from the other four. By reviewing the noise record of series B from March 23 to 27, it is understood that as most of the data points come from noise levels at around 58 dB, higher and lower noise levels have a relatively much smaller contribution. This is probably the reason why the slope of regression line is biased in this case. The average intercept is 30.4 ± 2.0 . The linear relation between the noise level (NSL) in dB re 1 μ Pa and wind speed (V) in knots can be expressed as Eq. (4.1)

$$20 \log V = 1.01 \text{ NSL} - 30.4 \quad (4.1)$$

Fig. 7 is a plot of wind speeds measured by R/V Researcher versus those computed from noise level series A in March by Eq. (4.1). The other three series, which have slopes of approximately 1.01, show similar figures and are not presented here. Data at low wind speeds do not distort the linearity in any of the cases observed.

Because the linear regressions were performed on variables with logarithmic scale, it is not easy to get the standard deviations directly; nevertheless, the deviation is estimated from Fig. 7 to be less than 5 knots at wind speeds between 5 and 25 knots. Since high wind conditions are scarce in the data, further experiments could refine the exact slope. However, there is no doubt about the existence of a linear relationship.

Since the slope in Eq. (4.1) is very close to 1, an alternate form of expression for the relationship between wind speed (V) in knots and the rms pressure of noise (p) in μ Pa is:

* In their case, the wind speed is the independent variable and the noise level is the dependent one.

$$V = 0.0302 p \quad (4.2)$$

To eliminate the error caused by de-emphasizing high wind conditions with a logarithmic scale in Eq. (4.1), Eq. (4.2) is suggested for performing the linear regression in future applications.

4.3 Wind speed calculations

Table 4 lists the mean values of wind speeds calculated from various noise level series. Only series C and G, which were measured by the same instrument, have mean values which agree well with the mean wind speeds from records of the R/V Researcher. Wind speed calculated from series E is 25% too low while the ones from series D and H are 30% too high. These disagreements have very likely resulted from the different gains of the instruments. Since the original purpose of IES noise measurement was not monitoring of wind speed, those instruments were not carefully calibrated and it is now impossible to get the correction factors for each IES.

Figs. 8a-f show the probability density functions of wind speeds calculated from noise levels and those observed by R/V Researcher. The fact that the whole curves as well as the mean values for D and H are translated to higher winds leads support to the assertion that those instruments merely had a higher gain than represented by Eq. (4.1). There may be some evidence of ship or self noise contribution, because the calculated probability density functions have no contribution in the lowest box, whereas the observed winds do have some probability of wind speed less than 3 to 6 knots. So 6 knots might be the lower limit for the wind speed determination of 5 kHz.

4.4 Stress estimation from noise measurements

Using Eq. (4.1) to calculate the surface wind speeds from the noise spectrum levels, the wind stress may then be computed. A quadratic resistance law, which comes from a dimensional consideration in the turbulent boundary layer theory, is used in the computation:

$$\underline{\tau} = \rho C_D |\underline{v}| \underline{v} \quad (4.3)$$

Here $\underline{\tau}$ is the stress vector in dyne/cm²; ρ is the density of air close to the sea surface in gm/cm³; C_D is the drag coefficient; and \underline{v} is the wind velocity at the 10 m or deck level while $|\underline{v}|$ is the magnitude of the wind velocity.

The average air density used by Hellerman (1967) was 1.20×10^{-3} gm/cm³ at latitude 28° N. The value of C_D varies according to different authors (Roll, 1965; Kraus, 1972). It also depends on many factors which are not yet well known. Sethuraman and Raynor (1975) found C_D to be 0.69, 1.06 and 1.75×10^{-3} for smooth, moderately rough and fully rough sea surface conditions respectively. The mean drag coefficient under unstable air stratification is about 10% higher than that under neutral conditions. A complete knowledge of the air density stratification and the roughness of sea surface is necessary for a good estimate of C_D .

In a study of wind stress over the North Atlantic Ocean, Bunker (1976) used C_D as a function of wind speed and air stability varying from 1.0×10^{-3} to 3.4×10^{-3} . Recent measurements show that his values may be too high (Dunckel et al, 1974; Ching, 1975; Smith and Banke, 1975), and the wind speed dependence is not significant (Demian and Miyake, 1973; Dunckel et al, 1974). The wind speed dependence of the drag coefficient may be significant only under hurricane conditions. Under most oceanic conditions, the sea surface is in the range of moderately rough to fully

rough (Sethuraman and Raynor, 1975), and the correlation of C_D for air stability is less than 10% (Hsu, 1974). Compared to the scatter of measured values of drag coefficient by different authors, the corrections for air stability or surface roughness are unimportant. During the whole MODE-I, the wind speed was hardly over 35 knots, so a constant C_D value of 1.5×10^{-3} has therefore been used.

By using Eq. (4.3), series of wind stress at all IES sites are derived. Fig. 9 shows the probability density functions of computed wind stress magnitude of series C and G which came from the same and best calibrated instrument. With wind directions supplied by R/V Researcher, mean wind stress ($\bar{\tau}$) of each month can be calculated from vector-averaging the individual stress (τ_i) by the equation

$$\bar{\tau} = \frac{1}{N} \sum_{i=1}^N \tau_i \quad (4.4)$$

The east and north components of the monthly mean wind stress are shown in Table 5. The stress obtained from series C and G are considered to be good estimates of mean wind stress during MODE-I. The number in each parenthesis is mean wind stress interpolated from Hellerman's table (1967). The values we obtained are generally higher than Hellerman's at the same region in spring and summer. This is mostly caused by the difference in methods: Hellerman calculated mean wind stress from the frequency distribution of wind velocity, instead of Eqs. (4.3) and (4.4). In Bunker and Worthington's report (1976) only annual mean stress curves are given, which are not comparable to our results.

To demonstrate the bias in computing mean wind stress from climatological mean wind speed, the biased mean stress ($\bar{\tau}_b$) was calculated by Eq. (4.5) below, from 205 hours of data of series C in late March,

$$\bar{\tau}_b = \rho C_D \bar{V} \quad (4.5)$$

where \bar{V} is the mean wind velocity. It was found that the result of Eq. (4.4) was almost four times that of Eq. (4.5). This example shows that the way of obtaining mean stress by Eq. (4.5) is seriously biased.

Error estimates for the wind stress over the ocean are seldom made in the literature, probably due to the large uncertainty associated with these observations. As in other methods, ours is subject to the same uncertainty in C_D , about 50%. Wind speeds calculated from ambient noise levels were estimated to have less than 5 knot error at speed between 5 and 25 knots (section 4.3); this corresponds to about 50% error in V^2 . Thus although the wind speeds derived from ambient noise measurements have considerable uncertainty (70%), distinct advantages may be realized from the continuous recording capability, and the relatively unbiased results.

Chapter 5

POWER SPECTRA AND COHERENCES OF RMS NOISE PRESSURES

The equivalence of ambient noise pressure with surface wind speed makes it possible to interpret the power spectral density functions and the coherences of surface wind speeds at pairs of localities 100 to 250 km apart. The power spectral density functions calculated from rms noise pressure series represent those of wind speeds and may be different from the spectra of wind velocity components. The calculation of velocity spectra involves the wind direction which was not available from ambient noise measurements, so only wind speed spectra were calculated.

Although the time series of March and April are strongly influenced by the passage of several energetic events, the standard spectral analysis techniques which strictly apply only to stationary time series, have been used. The cross-correlations between IES sites were also calculated to demonstrate the passage of fronts.

5.1 Power spectral density functions

The standard Fast Fourier Transform was performed on the rms noise pressure series with data length longer than 512 hours, after the mean values and linear trends were removed. For computational efficiency, shorter series in March and April were extended with zeroes to 512 hours. One tenth of each end of the original data was modified by a cosine taper window to prevent distortion of the power spectral estimates by leakage (Hannan, 1970). The smooth spectra were estimated from frequency band averaging (Bendat and Piersol, 1971). For those 512 hour series (A, B and C), eight adjacent frequencies were averaged and for

1024 hour series (D, E, G and H), sixteen were used.

Figs. 10a-d are the plots of power spectral density functions. The bar on the right-hand corner of each figure represents the 95% confidence interval. The spectra are generally monotone and featureless. Most power lies at the lower frequency end.* No significant peaks exist in this frequency range. This is in agreement with the wind speed spectra over the ocean for this latitude (Byshev and Ivanov, 1969).

5.2 Coherence functions

The cross-spectral density functions were computed from the Fourier coefficients. The amplitudes and phases of coherence functions were then derived from these spectra by the same frequency average method and shown in Figs. 11a-f. The 95% confidence level for rejecting zero hypothesis is given in each amplitude plot. The 95% confidence intervals for amplitude and the phase are dependent on the coherence at each frequency (see Koopmans (1974) or the table of Amos and Koopmans (1963)). The uncertainty of the A-C coherence phase is given in Fig. 11b as an example, but the error bars are left off the others for figure clarity.

Due to the difference in weather conditions, the coherence in those two sets of noise measurements are discussed separately. In March and April, the southeastward frontal movements result in coherence among all three noise series A, B and C (Figs. 11a-c). The coherence is significant at the 90% level ** for frequencies less than 0.3 C.P.H.. For some cases, the coherence is significant at the 95% level. At frequencies lower than

* On a log-log plot, the slope would be approximately -1.4 to -1.6.

** The coherence level of rejecting the zero hypothesis at 90% level is 0.53 and 0.38 for 16 and 32 degrees of freedom respectively.

0.1 C.P.H. and between 0.14 to 0.3 C.P.H., series A and B, which are closest to each other (100 km, see Fig.1) become coherent. For series B and C, which have the largest separation (250 km), the coherence is significant only in the frequency band of 0.15 to 0.25 C.P.H.. At the low frequency end, no coherence is found for B and C. Series A and C (190 km apart) have high coherence for both high and low frequency regions. All the phases in the coherence plots of Figs. 11a-c are linear functions of frequency. This corresponds to a constant time lag $S/2\pi$ between two series of noise measurements, where S is the slope on the phase plots (Koopmans, 1974); it agrees with the time lag for propagation of fronts between sites in March and April.

In May and June, no organized wind systems passed through the MODE area. The noise series D, E, G and H are not coherent at the 95% level and the phase angles are random.

Because the noise is affected mostly by local wind, the coherence among IES sites separated by several hundred kilometers can only arise from coherence in the wind field or from movement of organized atmospheric disturbances such as fronts or squall lines. Therefore, coherency further supports the assumption of the existence of the noise-wind relationship.

5.3 Correlation functions of rms noise pressures

Since the result of the coherence study may be dominated by several energetic processes which are not stationary random processes, the correlation functions are also computed to demonstrate the reliability of the above result.

Beginning on March 25, 406 hours of data from noise series A, B and C were used for correlation study. The resulting correlation functions

are plotted in Fig. 12. For all three series, a high correlation coefficient and a sharp peaked maximum exist. The correlation decreases to zero at a lag of around 30 hours. The movement of weather fronts passing the IES sites gives these sharp peaked maxima. The mean velocity of the atmospheric disturbances can be estimated from the lag time to be 30 km/hr southeastward. This agrees well with the surface weather maps.

The relative locations of IES's determine the magnitude of the correlation coefficients. Series A and B were measured at two sites 100 km apart in the typical direction of frontal movements (Fig.1). They give a much higher correlation coefficient than that of series A and C measured at sites 200 km apart in the north-south direction (Table 6). The time lags among them coincide with the ones given by the coherence phase slopes (section 5.2, Figs. 11a-c). The four noise series, of May and June with a common time interval of 948 hours beginning May 18, have low correlations (Table 6). The correlation functions again confirm the result of the coherence study.

Chapter 6

APPLICATION REMARKS

The results of this work show that recording the acoustic ambient noise levels gives promise as a good method in the open ocean for monitoring wind speed and stress variations. However, several factors may influence the ambient noise level at a specific location for a given wind speed: sound refraction and ray paths, the bottom reflectivity effects and even uncertainties in the empirical equation. This chapter suggests some experiments to investigate the practicality of applying this method widely, or at some long-term monitoring stations. The wind directions we used came from the records of R/V Researcher, but in practical uses no ship will stay close to the IES. The determination of wind direction, the variabilities of noise measurements, the uncertainty associated with the derivation of wind speed and wind stress, and the estimation of the rate of rainfall are discussed in this chapter.

6.1 The estimation of wind stress direction

The ambient noise measurement can not provide any information about wind direction. That must be determined independently. Surface pressure charts are available from National Climatic Center at six hour intervals. The access to this information is easy and the method used is simple. Aside from a small ageostrophic deviation, the wind direction is approximately parallel to the isobars. The estimate is fairly good at places with a prevailing wind direction such as in the westlies; however, it is not applicable near the equator or when the winds are rapidly changing (as at fronts). For areas where the above method is not

appropriate, the estimation of wind velocity can be done by tracking cumulus cloud movements from geostationary satellite pictures. This method has been used recently by several authors in tropical regions (Hubert and Whitney, 1971; Fujita et al, 1975; Hubert, 1976; Smith and Hasler, 1976). Cumulus clouds are tracked to estimate the wind velocity at nearly 850 mb (about 1500 m). The cumulus cloud motion does not necessarily coincide well with the wind velocity at that level, however, the direction of the wind may be adequately determined from satellite photographs. A deviation of 2.5° in determining the direction of cloud movement was claimed by Smith and Hasler (1976); however, additional small errors caused by the difference of cloud movement from the ambient wind can be expected. In order to get the surface wind direction from the wind direction at 850 mb, a geostrophic wind approximation is made: the surface wind direction is obtained by adding a correction angle* (ageostrophic deviation) to the direction at 850 mb (Petterssen, 1953). This method will be able to give wind direction satisfactorily for practical application.

6.2 Uncertainty associated with the deviation of wind speed and stress

(1) Variability of the ambient noise level

This variability, which comes from sources other than wind and is not detectable, gives the largest uncertainty in the determination of wind stress from ambient noise measurements. Other noise could be produced by local sources, such as passing ships and precipitation. The precipitation noise will be discussed in section 6.3. Ship generated

* Typical deviation between the wind at anemometer level and the geostrophic wind is from 15° to 35° .

noise in this frequency range should never be a problem except in a busy shipping lane. However, all other background variables mix together and the variability in ambient noise is inevitable.

From Perrone's (1976) work at 3 kHz, error estimates can be made from the standard deviation of noise levels at various wind speed conditions. At a wind speed as high as 40 knots, the standard deviation is 1 dB which corresponds to an error of 10% of the calculated wind speed (see Eq. (4.1)). The standard deviation is 2 dB at 20 knots. This will cause an error of 10 to 20% of that calculated wind speed. At speeds lower than 10 knots, the standard deviation, which is 2 to 3 dB, will give a serious error in the calculation of wind speed. However, using higher frequency noise such as in our study, this is probably not a limitation.

(2) Instrument error

Although in this experiment, the unknown gain offsets between instruments were up to 2 dB or even higher and limited some of the analyses, with an improvement of the circuitry and a consistent calibration of all instruments the error can be reduced to between 1 and 1.5 dB.

(3) Errors involved in the determination of the empirical equation

Eq. (4.1) is derived empirically from limited data. For other cases, the coefficients should be slightly modified to get a best-fit. Since the nature of the logarithm over-emphasises the low wind speed portion of the regression analysis, the associated errors cause unnecessary problems. The slope of 1.0 in Eq. (4.1) suggests that wind speed is proportional to the rms noise pressure. In an area where good wind observations are made, one should calculate the proportionality

constant of Eq. (4.2) directly. In this way, the accuracy of the wind speed calculation can be increased and the effects upon the noise level caused by sources other than wind can be reduced.

6.3 Estimation of the precipitation rate over the ocean

Rain can dramatically increase the underwater noise level, depending upon the rate of rainfall. Franz (1959) studied both theoretically and experimentally the noise produced by individual water droplets falling upon a water surface. He found a nearly "white" spectrum between 1 to 10 kHz, very different from the rain-free spectrum (Fig.13). Measurements made in Long Island Sound (Heindsman et al,1955) confirmed the "white" spectrum.

The difference between spectrum shapes of wind-generated noise and rain-generated noise potentially allows the distinction between these two. The rainfall rate could be estimated by comparing the precipitation noise with the value predicted from the model of Franz (1959). Franz's data shown in Fig. 13 indicates that even a fairly modest rate of rainfall (0.1 in/hr) would influence the ambient noise level. However, no measurement of rain noise at depths of 5000 m has been made. The contribution of precipitation noise to the total ambient noise level may decrease with increase in depth. Because the ship observed very little rainfall during MODE, the proportion of its contribution is not known in our study. Further experiments are needed to learn whether the rain noise and wind noise are distinguishable when both are measured at a great depth.

6.4 Future work

An important task for future applications is to test the scaling conversion of noise level to wind speed and wind stress in a variety of situations. The noise measurements are more appropriate in deep open ocean areas where the man-made and the biological sources are limited. As a preliminary step, several factors should be investigated:

- (1) During MODE, wind speeds over 30 knots were scarce. More studies are needed to verify Eq. (4.1) for use in conditions of high wind. Future tests and experiments should include seasons of different wind conditions to get the applicability of this method in both high and low wind conditions.
- (2) The ambient noise may be better related to wind stress than to wind speed. It has been recognized for some time that wave generation and the drag coefficient depend upon the air stratification above the water, as does ambient noise. In calculating wind stress from wind speed by using Eq. (4.3) with a constant drag coefficient, the effect of surface roughness is neglected. Since both the ambient noise and the drag coefficient are influenced by a common factor, the correlation of wind stress with ambient noise may be higher. To investigate this, direct measurements of wind stress by research vessels will be required for correlation with the ambient noise energy (mean squared pressure).
- (3) Any depth variation of the ambient noise could change the regression intercept or even the slope. Several well-calibrated IES's should be located nearby (say, 5 to 10 km) at different depths to find the depth effects.
- (4) The refraction effects due to the stratification of the sea

water may have an influence on the amount of wind generated noise penetrating into the deep water. This may result in a difference between equatorial regions and high latitude regions even when ice is not present.

- (5) The hydrophone for the ambient noise measurements will work better if it is nearly omnidirectional upward and the sensitivity is small in the downward direction. In this way, the effects of bottom reflection and the height off the bottom are negligible.
- (6) The rain noise can be studied by comparing the noise data with rate of rainfall to test the distinguishability of rain-noise from wind-noise. Two or more band pass filters (for perhaps, 2, 4 and 8 kHz) can be included in the circuit to perform this test.

These tests can be made in areas where extensive wind observations are available. One possibility is the BOMEX area where wind stress has been measured by various methods. It will then be easy to compare the result of noise measurement directly with wind stress measured by ships which is more objective than wind stress estimated from Eq. (4.3). Measurements of ambient noise can be made at localities of special interest. By comparing the empirical equations obtained from different areas, it can be determined if a universal equation is good for all studies or if some corrections are needed for each locality. Hopefully careful wind observations just after launching an instrument will serve to calibrate the equation for that site.

Chapter 7

SUMMARY AND CONCLUSION

Acoustic ambient noise levels at 5 kHz measured by seven Inverted Echo Sounders during MODE-I were examined to search for the relationship of noise level to the oceanic wind speed and wind stress. Because of the lack of surface wind speed information directly over each IES site, ambient noise records were compared with the wind speeds observed by the R/V Researcher during the same experiment. A linear regression equation, relating the observed wind speed (V) to the noise spectrum level (NSL), was determined as

$$20 \log V = 1.01 \text{ NSL} - 30.4$$

The wind speed calculated from this equation is actually a mean wind speed for an area within a radius of about 5 to 10 km around each noise measurement site, because sound refraction and attenuation in the ocean limit the distance from which noise sources can contribute significantly. The error in the wind speed estimation from this equation is less than 5 knots (~ 2.5 m/sec) at wind speeds 5 to 25 knots. This relationship should extend to higher noise levels and wind speeds.

The comparison of calculated mean wind speeds with the observed ones showed that several instruments were not well calibrated. Given good wind speed observations directly over the IES sites and well-calibrated instruments, the estimate could be refined to an accuracy restricted principally by the standard deviation of ambient noise levels at each wind speed, which is 10 to 20% for wind speeds higher than 20 knots and about 5 knots for low wind speeds. However, there are remaining questions which could change the above empirical

relationship depending upon geographic location, depth, sound refraction effects and sea bottom reflectivity, all of which could alter the additive constant (-30.4) or possibly even the slope. Studies in the literature have investigated some of these problems, for the purpose of determining ambient noise levels at lower frequencies (up to 3 kHz) from observed winds. This study inverts the problem, working at 5 kHz in deep water. The advantages at this frequency are that the noise sources must be more localized and the contamination by shipping noise must be less; this allows better accuracy than using low frequencies for the wind speed estimation. However, the lower noise spectrum levels which exist at high frequencies make the measurement more difficult and subject to rain-noise domination.

The seven time series of ambient noise were converted to wind speed records via the above equation in order to study statistical properties of the wind field during the MODE experiment and to estimate the wind stress. The probability density functions of wind speed and stress were constructed and the former is in agreement with those derived from the R/V Researcher wind speed information. The power spectral density functions of the rms noise pressures were found to decrease smoothly with increasing frequency consistent with other oceanic wind speed spectra found in the literature.

The wind field during March-April was characterized by organized weather fronts moving through the MODE area, as revealed by the coherent noise rms pressures between pairs of IES sites 100 to 250 km apart. Cross-correlation time lags between pairs of noise series determined the mean velocity of frontal movement to be 30 km/hr to the southeast. Surface weather charts from the National Climatic Center

agree with this result.

The calculated wind speeds were also used to compute the wind stress from the equation

$$\bar{\tau} = \rho C_D / 2 \bar{V}^2$$

where wind direction was determined from observations aboard the R/V Researcher. Whereas the wind stress values obtained are only representative of this location for a brief time period, they are generally higher than those found in the literature. In future experiments, the wind directions would have to be estimated from either surface pressure charts or tracking cloud motion by satellite. We foresee the following advantages with this method of recording wind stress: 1) the average wind stress may be calculated in the proper way from the squared wind speed instead of approximating it from the squared mean wind speed, and 2) it is not fair-weather-biased. The uncertainty is estimated to be 70% in the calculating individual values of wind stress from the ambient noise. However, the monthly mean values would deviate less from the true value statistically by performing the average.

Several future experiments have been suggested in Chapter 6. The applicability of the regression equation found above should be tested at a variety of locations, depths, wind conditions, air stratifications, and rates of precipitation. With this knowledge, the noise measurement may be widely applicable to study long-term wind stress and wind speeds, particularly in remote areas.

Appendix A

INSTRUMENT SPECIFICATIONS

The characteristics of the elements for ambient noise measurements in the Inverted Echo Sounder are described below. These elements include a transducer, pre-amplifier, 5 kHz amplifier, logarithmic peak detector, and voltage-frequency converter (Fig. 3).

(1) Transducer

The pinger which generates 5 kHz signals for retrieving the instruments was also used as the receiver for the 5 kHz ambient noise. It is separate from the main echo sounding transducer, and located below the instrument, i.e. not optimized for the ambient noise measurement. The frequency response of this 5 kHz transducer actually limits the band width of the noise measurement circuitry. It is a narrow band centered at 5 kHz with a 1 kHz band width as determined by -3 dB points. The directional response is shown in Fig. A1. It is almost omnidirectional with an equivalent directivity index 2.4 dB in the upper half of the solid angle in which direction the sound propagates directly from sources at the surface. The maximum sensitivity of the receiving response is measured as -176.5 db/ μ Pa re 1 volt in the horizontal direction (Fig. A2).

(2) Pre-amplifier

The frequency response of the pre-amplifier is fairly constant over a broad band. The gain is 25.3 dB with less than 3% variation over the frequency range 2 to 14 kHz.

(3) 5 kHz amplifier

It has a gain of 48.7 dB at 7 kHz and the -3 dB points

are at 3.5 and 12 kHz respectively. The uncertainty in the gain of the circuit from instrument to instrument is estimated to be 20% (2 dB), while the temperature variation is 0.03%/°C.

(4) Logarithmic peak detector (log detector)

The log detector is an envelope detector. The response is linear with an input voltage in the range from 12 mV to 4 V.

(5) Voltage-frequency converter (V-F converter)

The response is linear with an input voltage from 0 to -2 V.

Appendix B

THE INSTRUMENT CALIBRATION

The response of the system with transducer, pre-amplifier and 5 kHz amplifier is the sum of the frequency response of each element (Fig. B1). For an input 5 kHz noise level of NSL dB re 1 μ Pa/Hz, the output voltage per frequency band from the 5kHz amplifier is $NSL + (-176.5 - 2.4) + 25.3 + 48.7 = (NSL-104.9)$ dB re 1 volt/Hz. The system response is equivalent to a gain of -104.9 dB/ μ Pa re 1 volt/Hz, with a band width 1.4 kHz centered at 5 kHz. The output voltage, V , for this pass band after the 5kHz amplifier is:

$$V \text{ dB re 1 volt} = NSL + 10 \log 1400 - 104.9 = NSL - 73.4$$

where the term $(10 \log 1400)$ comes from the band width and -104.9 is the system gain. With a change of the reference voltage to that used in the instrument specification (400 mV/Peak-peak), the output voltage in dB re 400 mV/p-p is:

$$V' \text{ dB re 400 mV/p-p} = NSL - 73.4 - 20 \log(200/1000) = NSL - 59.4 \quad (B.1)$$

The typical ambient noise level in the ocean is from 30 to 80 dB re 1 μ Pa/Hz. The output from the 5kHz amplifier will be from -20 to +7 dB re 400 mV/p-p. From Appendix A, it can be seen that all these values are well within the linear region of log detector and V-F converter.

Fig. B2 is the relation of the input voltage of the log detector in dB re 400 mV/p-p with the recorded counts which are obtained from counting the variable frequency output of the V-F converter. Because each counting period is 24 seconds, Eq. (B.2) is found to express this relationship:

$$V' = -37.9 + 0.00561 \times \text{count} \quad (B.2)$$

Ambient noise spectrum level can then be calculated from Eqs.(B.1) and (B.2),

$$\text{NSL (dB re } 1 \mu\text{Pa/Hz}) = 21.5 + 0.00561 \times \text{count} \quad (B.3)$$

Eq. (B.3) is used in the calculation of noise spectrum levels from recorded counts.

BIBLIOGRAPHY

Amos, D. E. and L. H. Koopmans, 1963. Tables of the distribution of the coefficient of coherence for stationary bivariate Gaussian processes. Office of Technical Services, Dept. of Commerce, Washington D. C..

Axelrod, E. H., B. A. Schoomer and W. A. Von Winkle, 1965. Vertical directionality of ambient noise in the deep ocean at a site near Bermuda. *J. Acoust. Soc. Am.*, 37: 77-83.

Bendat, J. S. and A. G. Piersol, 1971. Random data: analysis and measurement procedures. Wiley-Interscience, New York.

Bunker, A. F., 1976. Computation of surface energy flux and annual air-sea interaction cycles of the North Atlantic Ocean. *Mon. Wea. Rev.*, 104: 1122-1140.

Bunker, A. F. and L. V. Worthington, 1976. Energy exchange charts of the North Atlantic Ocean. *Bull. Amer. Meteor. Soc.*, 57: 670-678.

Byshev, V. I. and Y. A. Ivanov, 1969. The time spectra of some characteristics of the atmosphere above the ocean. *Bull. (Izv.), Acad. Sci., USSR, Atmospheric and Oceanic Physics*, 5: 8-13.

Ching, J. K., 1975. Determining the drag coefficient from velocity, momentum and mass budget analyses. *J. Atmos. Sci.*, 32: 1898-1908.

Crouch, W. W. and P. J. Burt, 1972. The logarithmic dependence of surface generated ambient-sea-noise spectrum level on wind speed. *J. Acoust. Soc. Am.*, 51: 1066-1072.

Denman, K. L. and M. Miyake, 1973. Behavior of the mean wind, the drag coefficient and the wave field in the open ocean. *J. Geophys. Res.*, 78: 1917-1924.

Dunckel, M., L. Hasse, L. Krugermeyer, D. Schriever and J. Wucknitz, 1974. Turbulent fluxes of momentum, heat and water vapor in the atmospheric surface layer at sea during ATEX. *Boundary-Layer Meteorol.*, 6: 81-106.

Franz, G. J., 1959. Splashes as sources of sound in liquids. *J. Acoust. Soc. Am.*, 45: 1080-1096.

Frisch, W. L., 1966. Sea noise vs near and distant wave height and wind speed. U. S. Navy Electronic Lab., San Diego, Calif. Research and Development Report 1390.

Fujita, T. T., E. W. Fearn and W. E. Shenk, 1975. Satellite-tracked cumulus velocities. *J. Appl. Meteor.*, 14: 407-413.

Hannan, E. J., 1970. Multiple time series. Wiley, New York.

Heindsman, T. E., R. H. Smith and A. D. Arneson, 1955. Effect of rain upon underwater noise levels. *J. Acoust. Soc. Am.*, 27: 378-379.

Hellerman, S., 1965. Computations of wind stress fields over the Atlantic Ocean. *Mon. Wea. Rev.*, 93: 239-244.

Hellerman, S., 1967. An updated estimate of the wind stress on the world ocean. *Mon. Wea. Rev.*, 95: 607-626. (see: Correction of tables in *Mon. Wea. Rev.*, 96: 63-74. 1968)

Hsu, S. A., 1974. On the log-linear wind profile and the relationship between shear stress and stability characteristics over the sea (research notes). *Boundary-Layer Meteorol.*, 6: 509-514.

Hubert, L. F., 1976. The relation between cloud pattern motion and wind shear. *Mon. Wea. Rev.*, 104: 1167-1171.

Hubert, L. F. and L. F. Whitney, 1971. Wind-estimation from geostationary-satellite pictures. *Mon. Wea. Rev.*, 99: 665-672.

Koopmans, L. H., 1974. The spectral analysis of time series. Academic Press, New York.

Kraus, E. B., 1972. Atmosphere-ocean interaction. Clarendon Press, Oxford. p. 153.

Kuo, E., 1968. Deep-sea noise due to surface motion. *J. Acoust. Soc. Am.*, 43: 1017-1024.

Longuet-Higgins, M. S., 1950. A theory of the origin of microseisms. *Trans. Roy. Soc. (London)*, A 243: 1-35.

Marsh, H. W., 1963. Origin of the Knudsen spectra. *J. Acoust. Soc. Am.*, 35: 409-410.

Perrone, A. J., 1969. Deep-ocean ambient-noise spectra in the Northwest Atlantic. *J. Acoust. Soc. Am.*, 46: 762-770.

Perrone, A. J., 1970. Ambient-noise-spectrum levels as a function of water depth. *J. Acoust. Soc. Am.*, 48: 362-370.

Perrone, A. J., 1976. Summary of a one-year ambient noise measurement program off Bermuda. Naval Underwater Systems Center, New London Lab. Technical Report 4979.

Petterssen, S., 1956. Weather analysis and forecasting. 2nd ed., McGraw Hill, New York. p. 83.

Phillips, N., 1966. Large-scale eddy motion in the Western Atlantic. *J. Geophys. Res.*, 71: 3883-3891.

Piggott, C. L., 1964. Ambient sea noise at low frequencies in Shallow water of the Scotian Shelf. *J. Acoust. Soc. Am.*, 36: 2152-2163.

Pollard, R. T., 1973. The deepening of the wind-mixed layer. *Geophys. Fluid Dyn.*, V: 381-404.

Roll, H. U., 1965. Physics of the marine atmosphere. Academic Press, New York.

Rossby, H. T., 1973. Inverted Echo Sounder: a description and some results from MODE-I. *MODE Hot Line News*, 41, Oct 12, 1973.

Sethuraman, S. and G. S. Raynor, 1975. Surface drag coefficient dependence on the aerodynamic roughness of the sea. *J. Geophys. Res.*, 80: 4983-4988.

Smith, C. L. and A. F. Hasler, 1976. A comparison of low-cloud satellite wind estimates with analyses based on aircraft observations in a disturbed tropical regime. *Mon. Wea. Rev.*, 104: 702-708.

Smith, S. D. and E. G. Banke, 1975. Variations of the sea surface drag coefficient with wind speed. *Quart. J. R. Met. Soc.*, 101: 665-673.

Urick, R. J., 1975. Principles of underwater sound. 2nd ed., McGraw Hill, New York.

Watts, D. R. and H. T. Rossby, 1976. Measuring dynamic heights with Inverted Echo Sounders: results from MODE. Submitted to *J. Phys. Oceanogr.*

Wenz, G. M., 1962. Acoustic ambient noise in the ocean: spectra and sources. *J. Acoust. Soc. Am.*, 34: 1936-1956.

Table 1 Mean wind speeds and standard deviations from ship observations

Month	Data length in hours	Mean wind speed in knots	Standard deviation	Maximum wind speed in knots
March	456	14.8	7.6	40
April	480	14.9	7.4	32
May	500	10.9	4.1	24
June	480	12.0	3.9	21

Table 2 Peak-cross correlation coefficients between noise and wind speed *

noise month series	A	B	C	D	E	G	H
March	0.69 (-6) (71)	0.69 (-2) (133)	0.63 (-11) (205)	-	-	-	-
April	0.76 (-1) (125)	0.73 (+3) (125)	0.77 (0) (480)	-	-	-	-
May	-	-	-	0.42 (-4) (378)	0.45 (+6) (378)	0.50 (+12) (378)	0.45 (-4~+9) (378)
June	-	-	-	0.58 (0) (480)	0.65 (-1) (480)	0.63 (+1) (480)	0.31 (+1) (480)

* For each column of three numbers, the first one is correlation coefficient, the second is the number of hours by which noise leads wind, the third is the length of data in hours.

Table 3 Least-square regression coefficients

Month	Noise series	Data length	Mean noise (dB re 1 μ Pa)	Mean wind speed (knots)	Intercept	Slope	F
March	A	71	54.6	18.6	-28.7	1.00 ±0.09	64
"	B	133	57.0	21.1	-18.2	1.29 ±0.12	121
"	C	205	53.5	17.6	-28.8	0.99 ±0.12	130
April	A	120	52.5	12.6	-31.5	1.02 ±0.08	181
"	B	120	53.7	12.6	-32.5	1.02 ±0.09	116

Table 4 Mean wind speeds and standard deviations calculated from ambient noise levels

Month	Noise series	Data length in hours	Mean wind speed in knots	Standard deviation
April	C	480	15.6	\pm 5.1
June	D	480	17.1	\pm 3.9
"	E	480	9.2	\pm 2.6
"	G	480	12.7	\pm 3.8
"	H	480	15.8	\pm 3.6

Table 5 Monthly mean wind stress derived from noise series*

Month	Noise series	Wind stress τ (dyne/cm ²)			
		x component	y component	$ \tau $	θ (degrees from true north)
April	C	-0.69 (-0.17)	-0.49 (-0.01)	0.85	234
June	D	-1.0 (-0.32)	0.16 (0.08)	1.01	279
"	E	-0.33 (-0.39)	0.03 (0.03)	0.33	275
"	G	-0.65 (-0.29)	0.04 (0.10)	0.65	274
"	H	-0.78 (-0.21)	0.02 (0.13)	0.81	284

* The number in each parenthesis is the value interpolated from Hellerman's tables (Hellerman, 1967)

Table 6 Maximum cross-correlation coefficients between noise level series

	A [*]	B [*]	C [*]	D ^{**}	E ^{**}	G ^{**}	H ^{**}
A	1.0 (0)	0.78 (-3.0)	0.62 (+5.0)	-	-	-	-
D	-	-	-	1.0 (0)	0.43 (-7)	0.51 (-3)	0.48 (-4)

* April series; data length 406 hours

** May-June series; data length 948 hours

The number in each parenthesis is the lag time in hours.

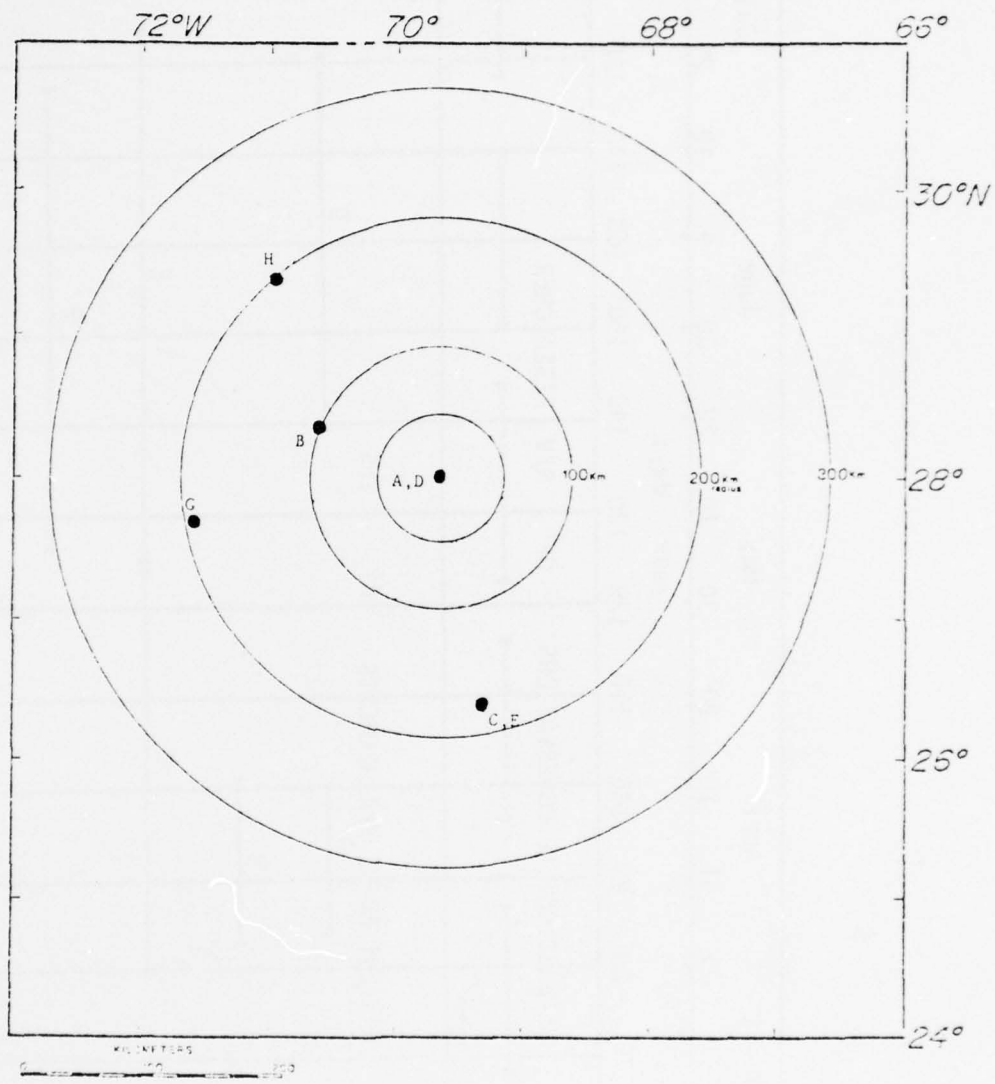


Fig. 1 Positions of Inverted Echo Sounders during MODE-I

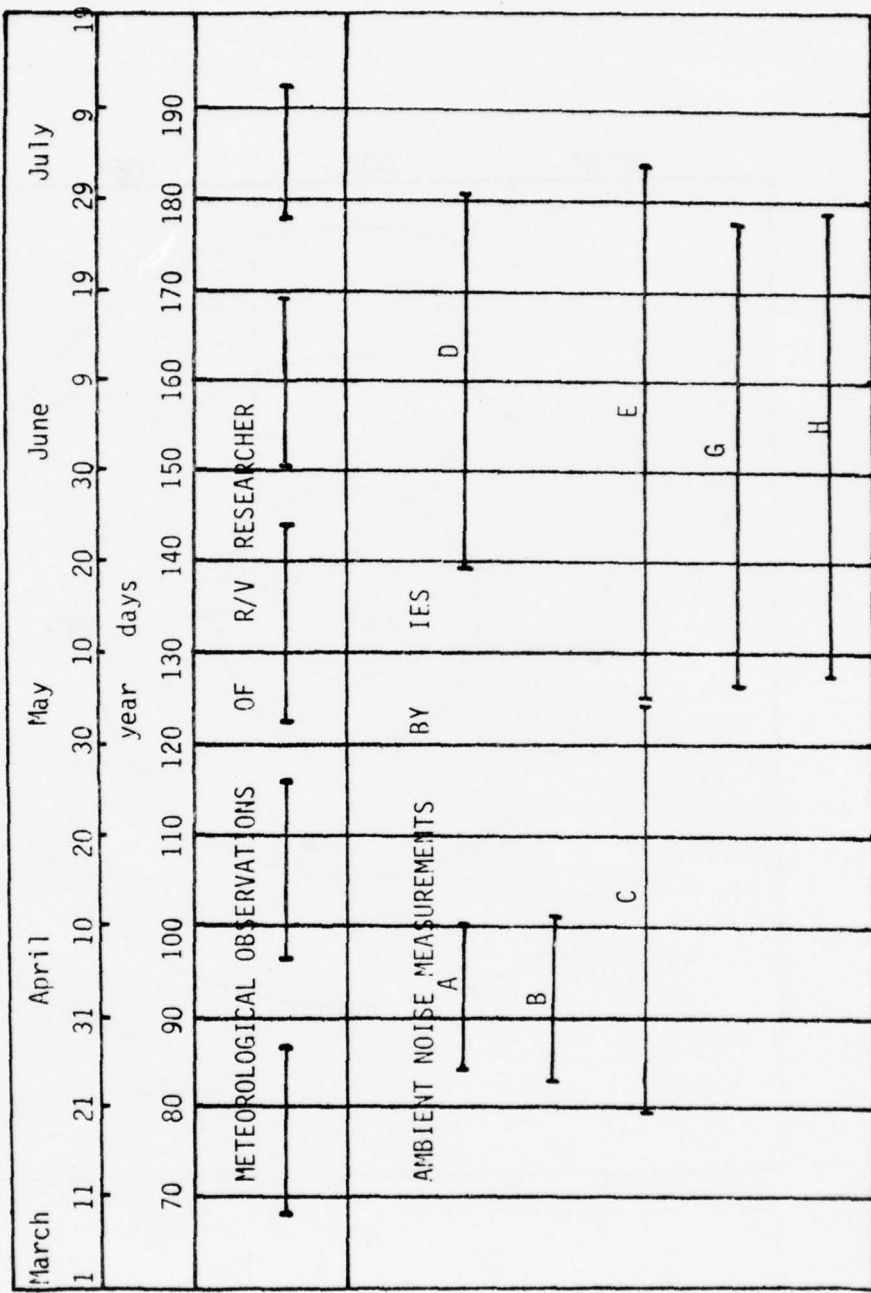


Fig. 2 Duration of ambient noise measurements and wind speed records during MODE-I

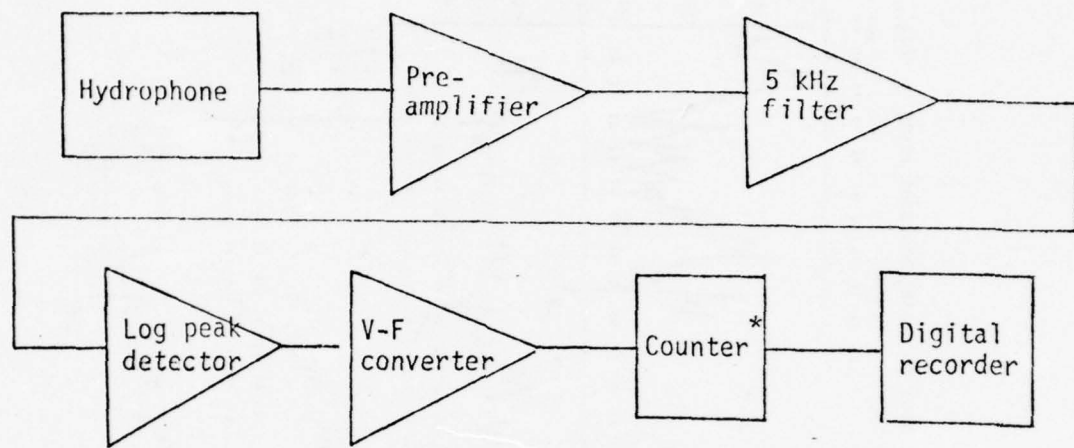


Fig. 3 Block diagram of IES noise measurement

* Every four minutes, the counter operates for twenty-four seconds.

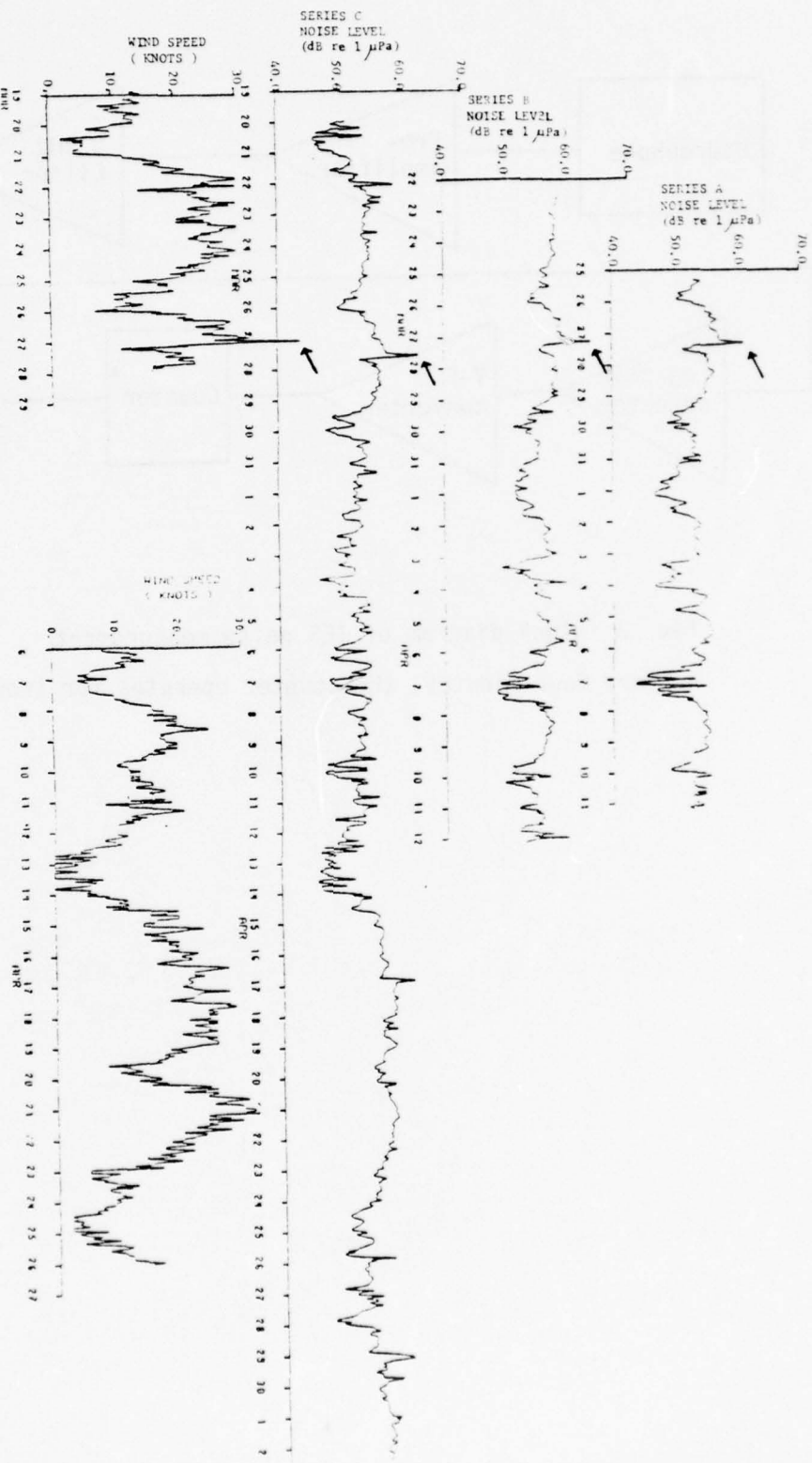


Fig. 4 Noise spectrum levels at three IES sites and wind speed of the same period observed by R/V Researcher

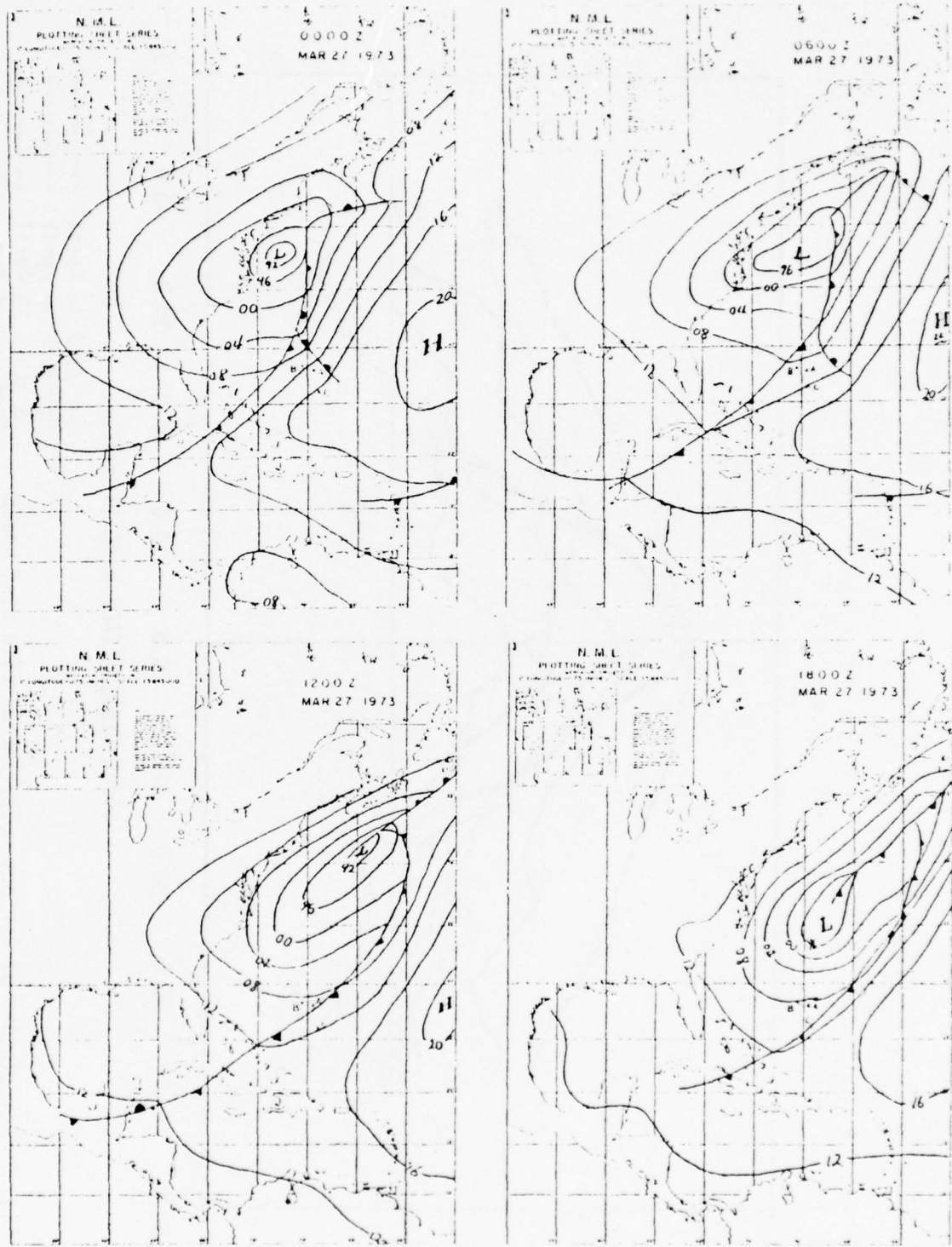


Fig. 5 Six-hour synoptic sea level pressure maps, March 27, 1973

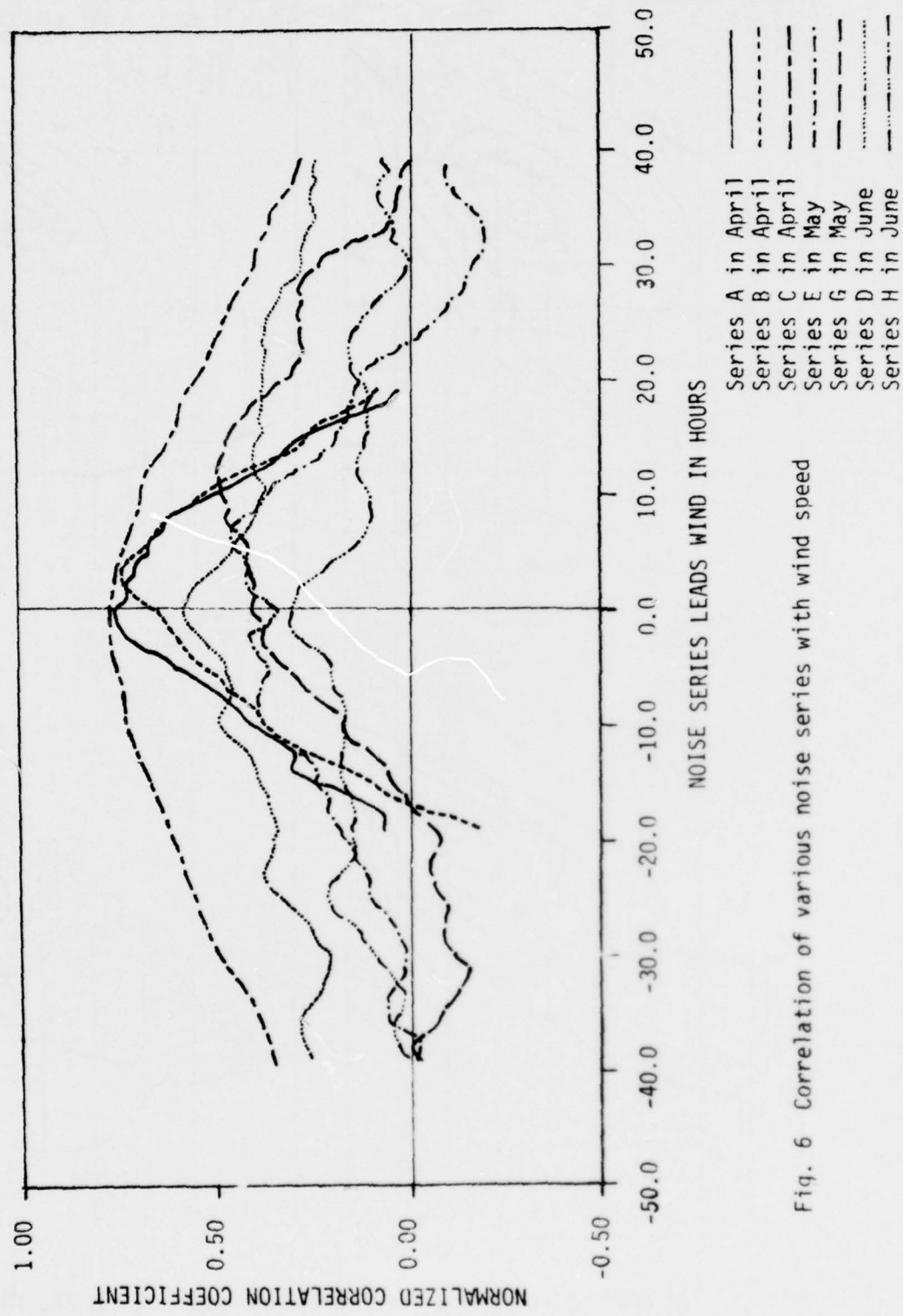


Fig. 6 Correlation of various noise series with wind speed

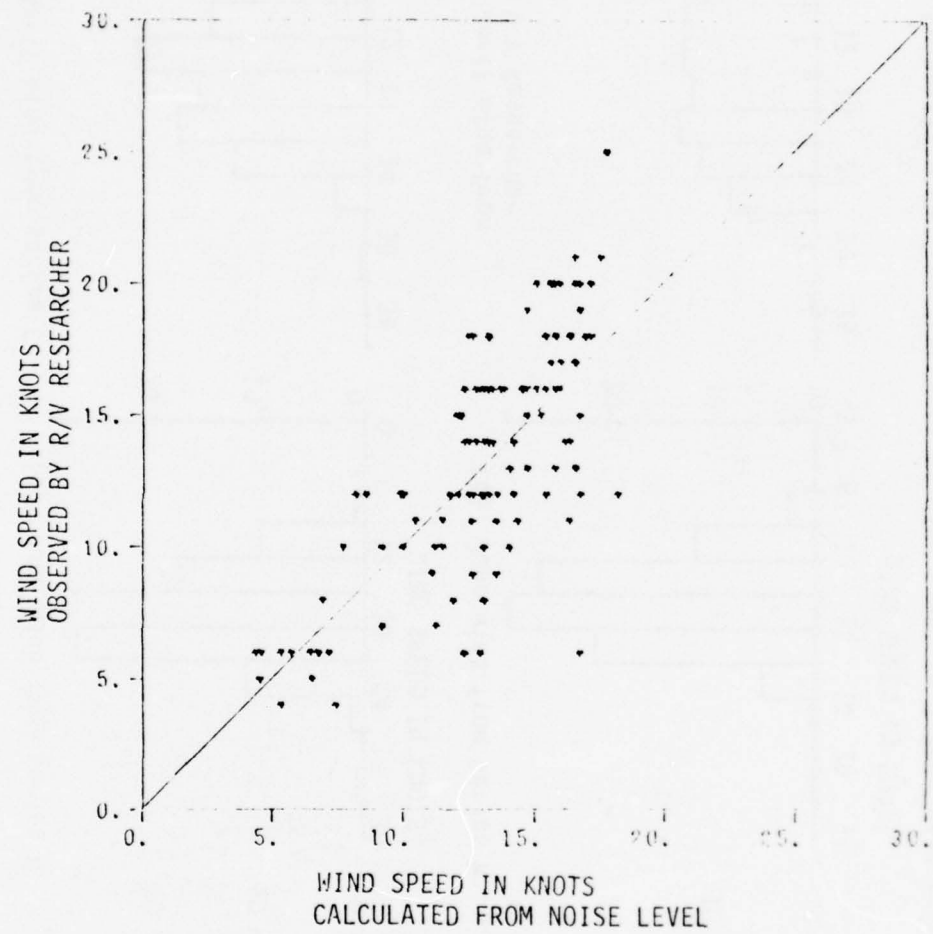


Fig. 7 Wind speed observed versus wind speed derived from ambient noise measurement of IES at site A

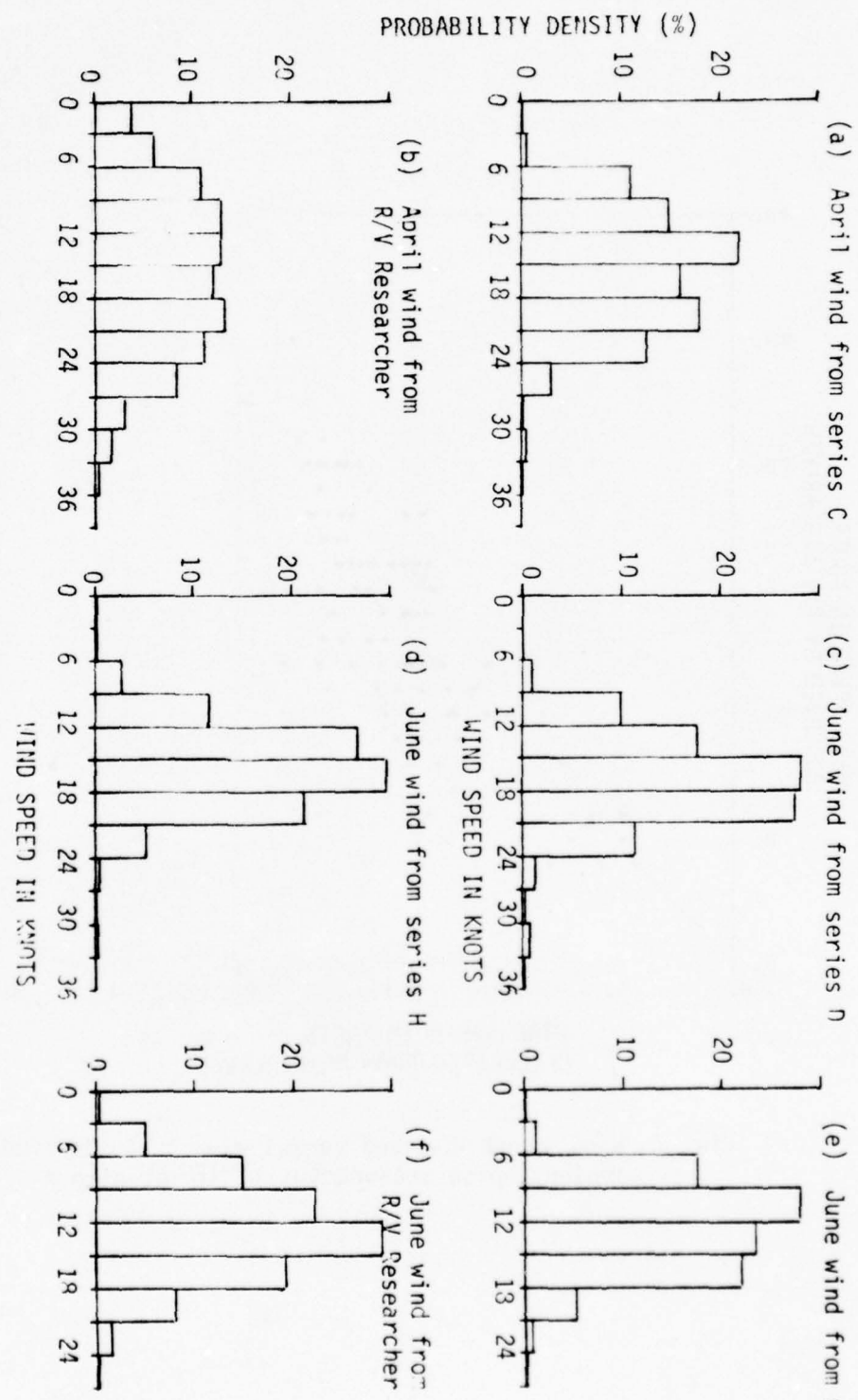


Fig. 3 probability density functions of wind speed in 3-knot wind speed groups

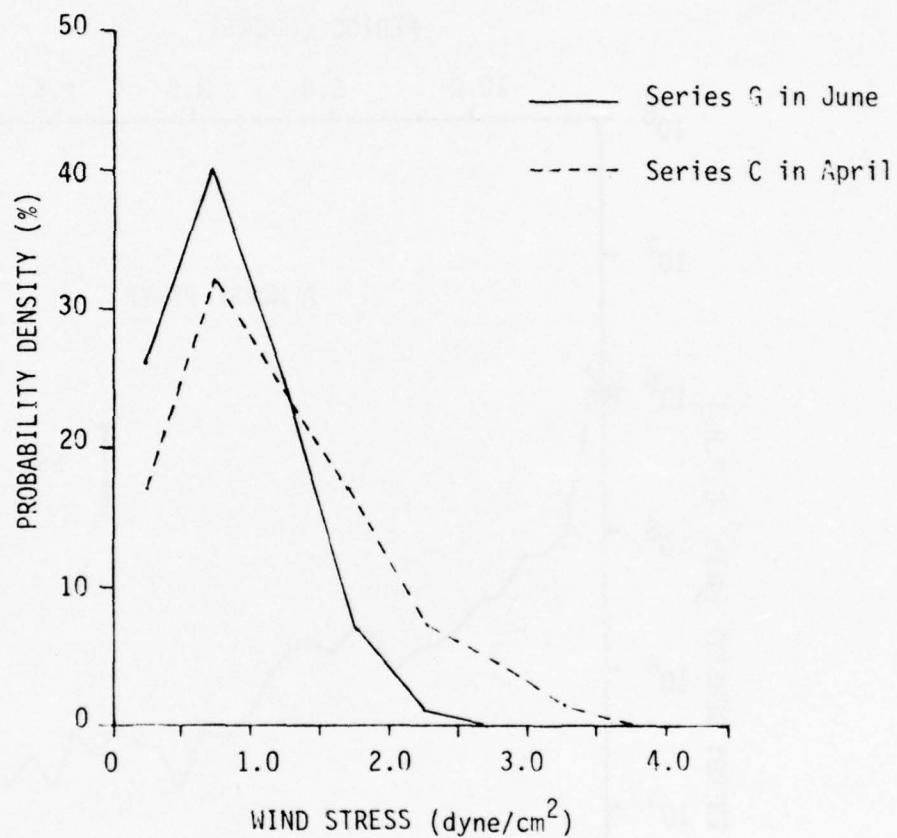


Fig. 9 Probability density functions of wind stress
in 0.5 dyne/cm² groups computed from noise level
series C and G

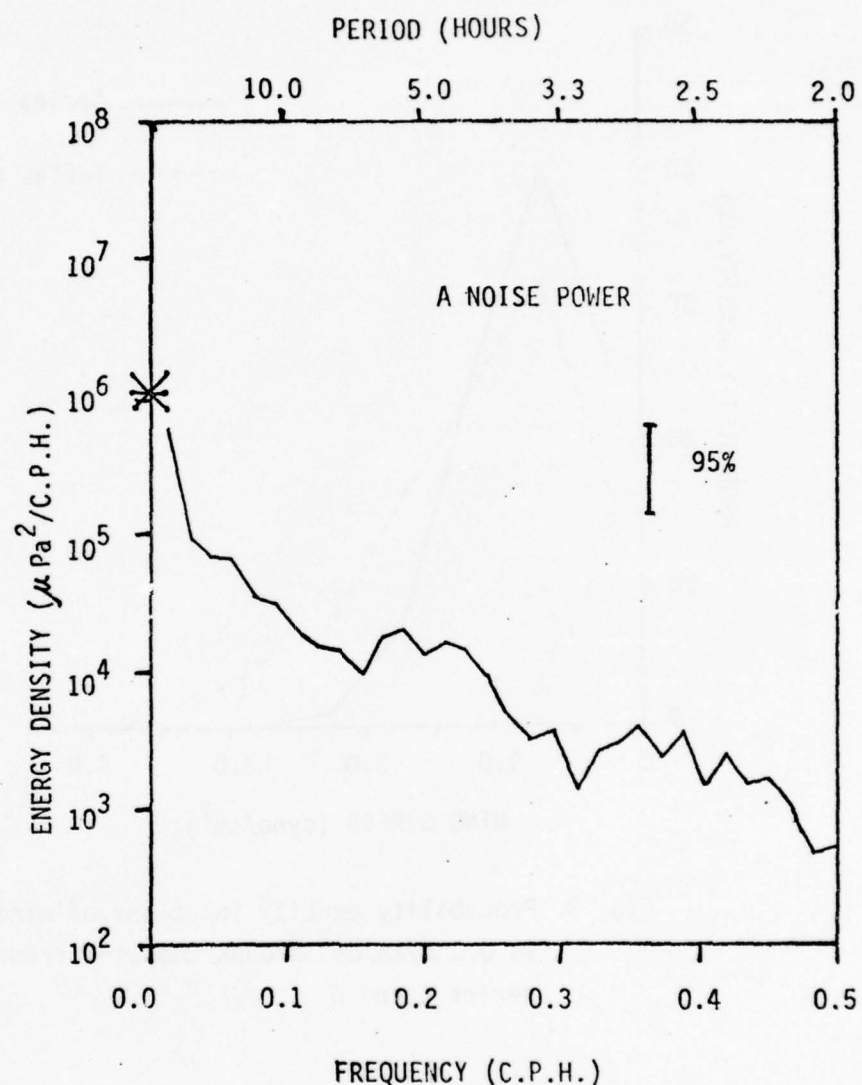


Fig. 10a Power spectral density function of noise pressure series A (March 25 - April 11)

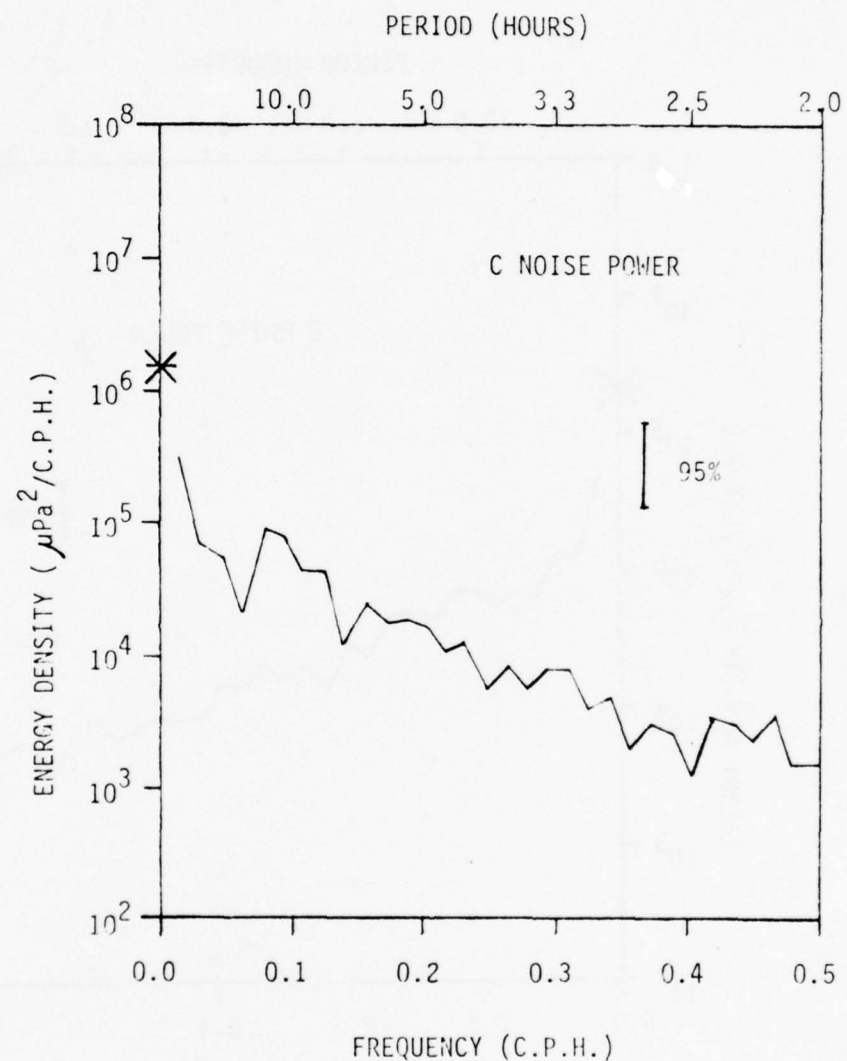


Fig. 10b Power spectral density function of noise pressure series C (March 25 - April 11)

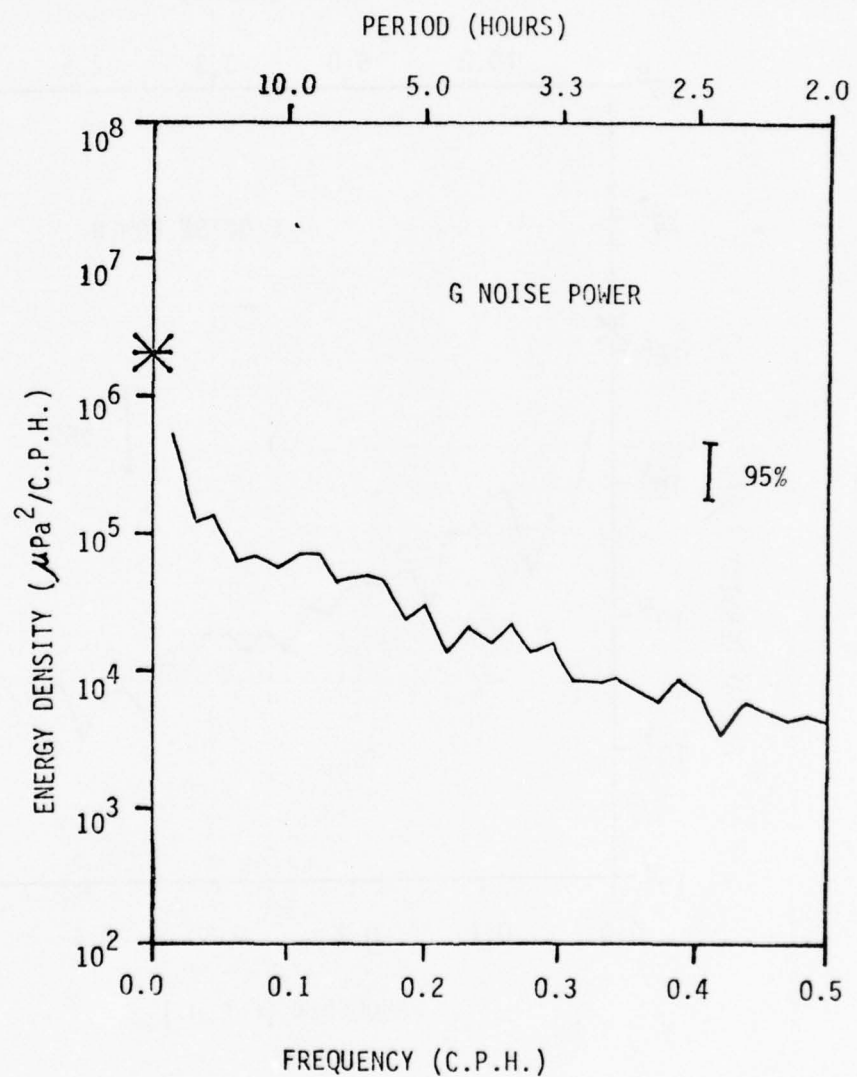


Fig. 10c Power spectral density function of noise pressure series G (May 7 - June 18)

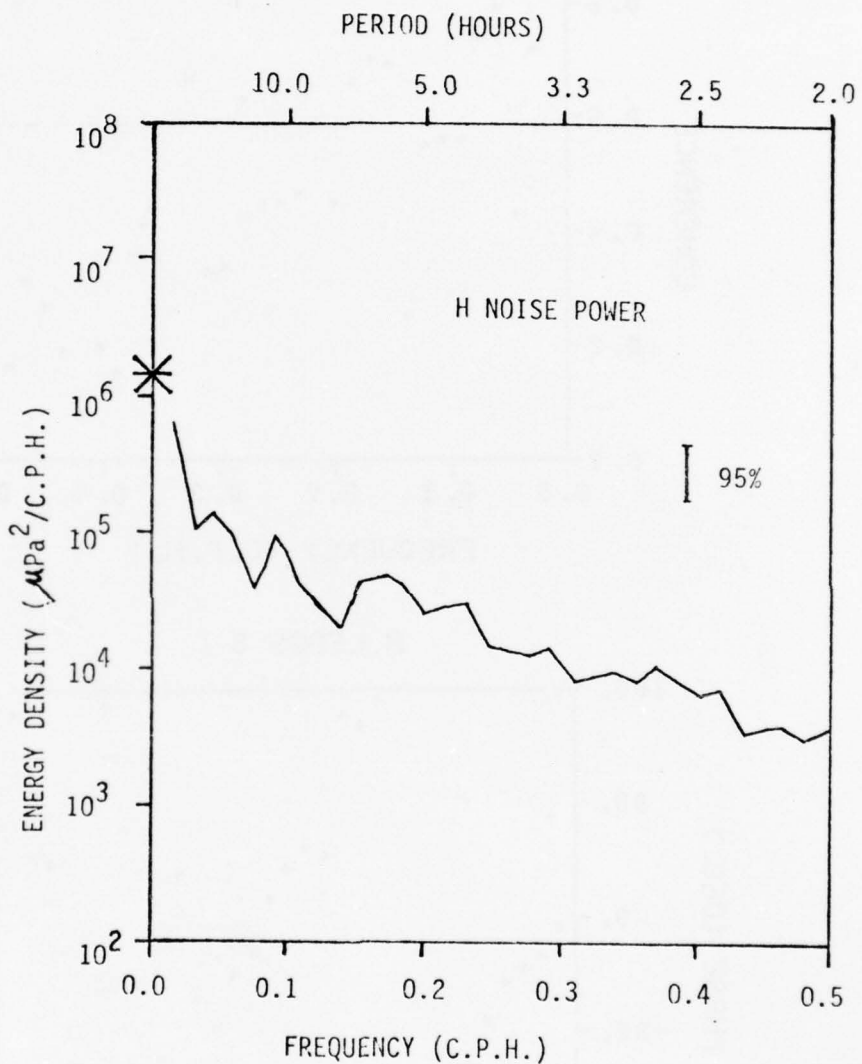


Fig. 10d Power spectral density function of noise pressure series H (May 7 - June 18)

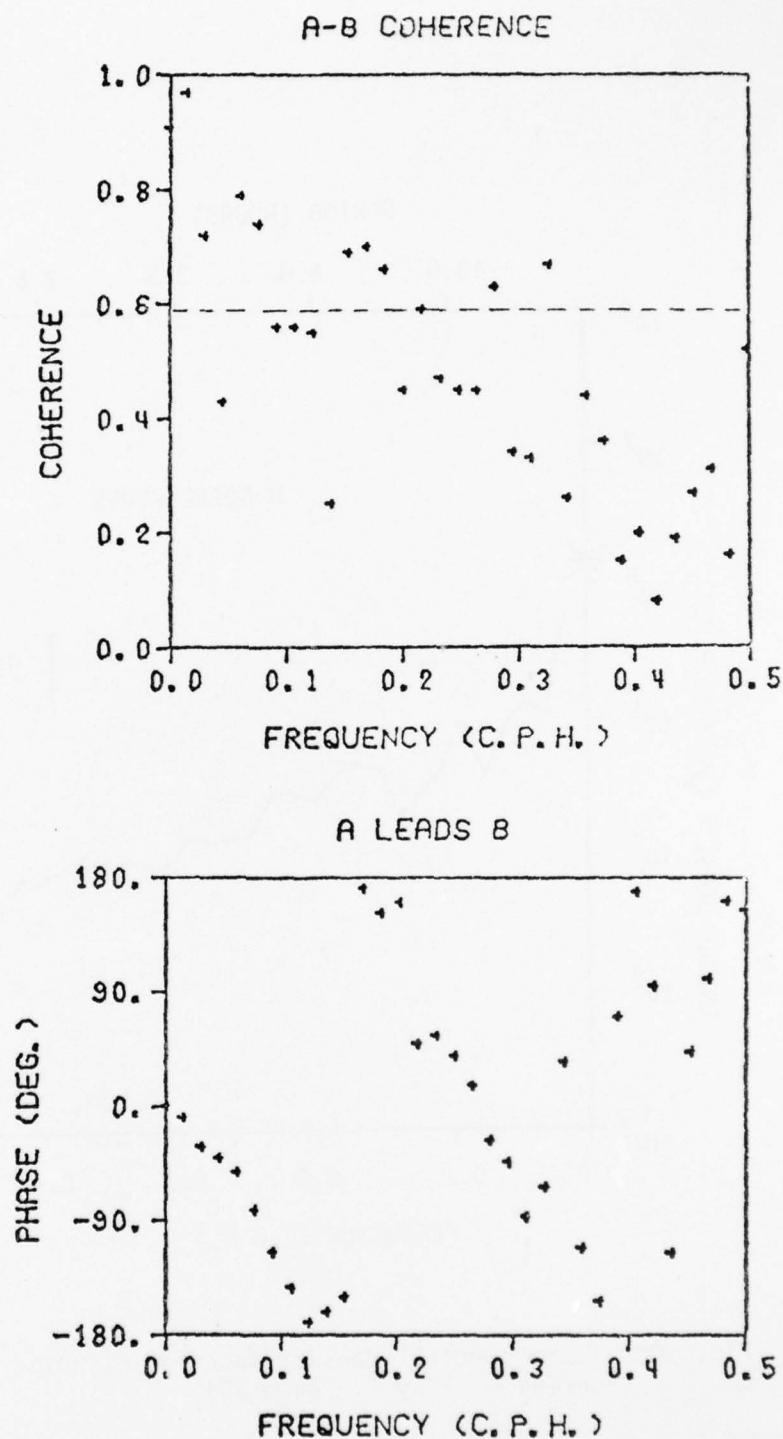


Fig. 11a Coherence between noise series A and B
from March 25 to April 11

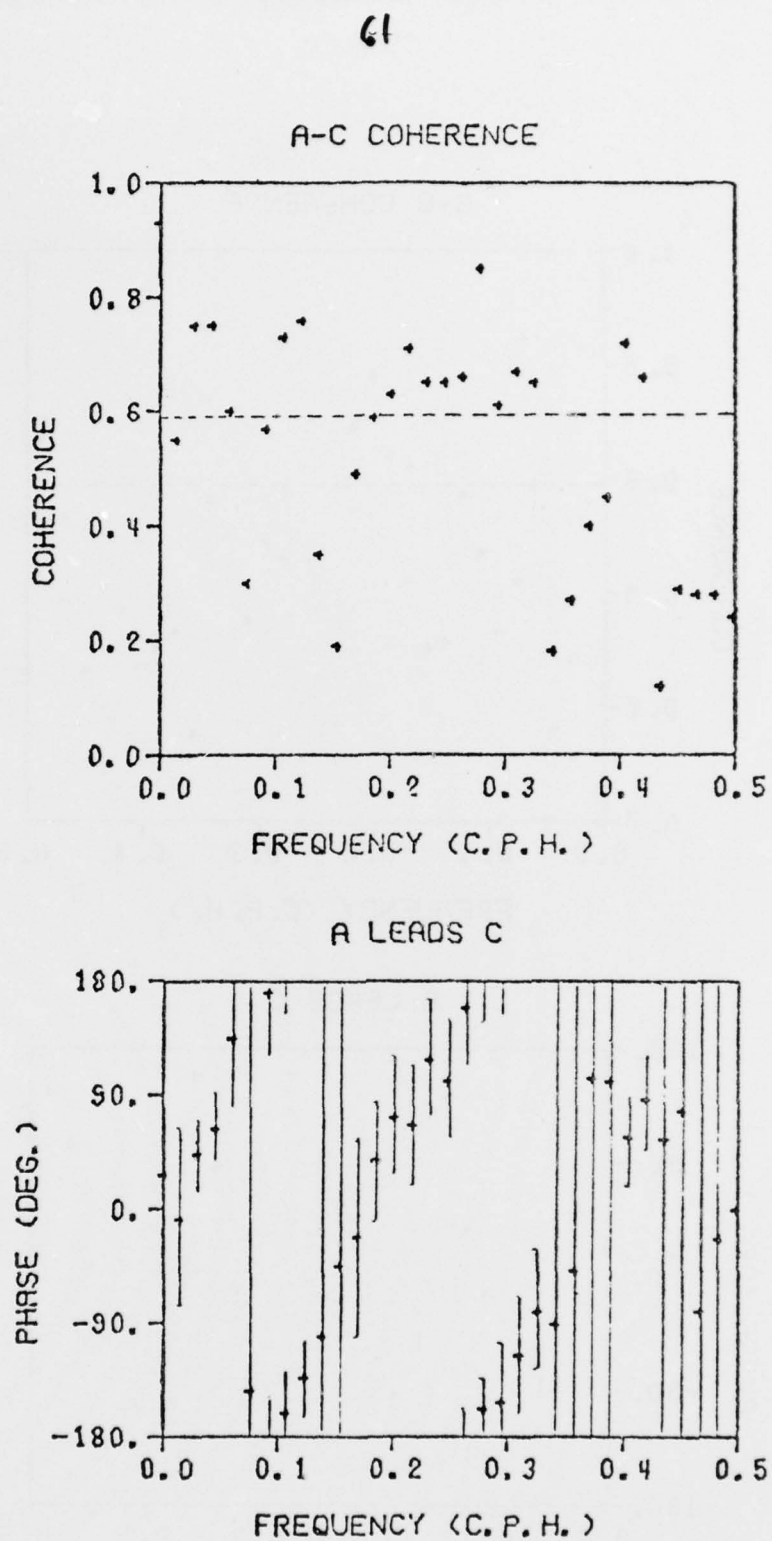


Fig. 11b Coherence between noise series A and C
from March 25 to April 11

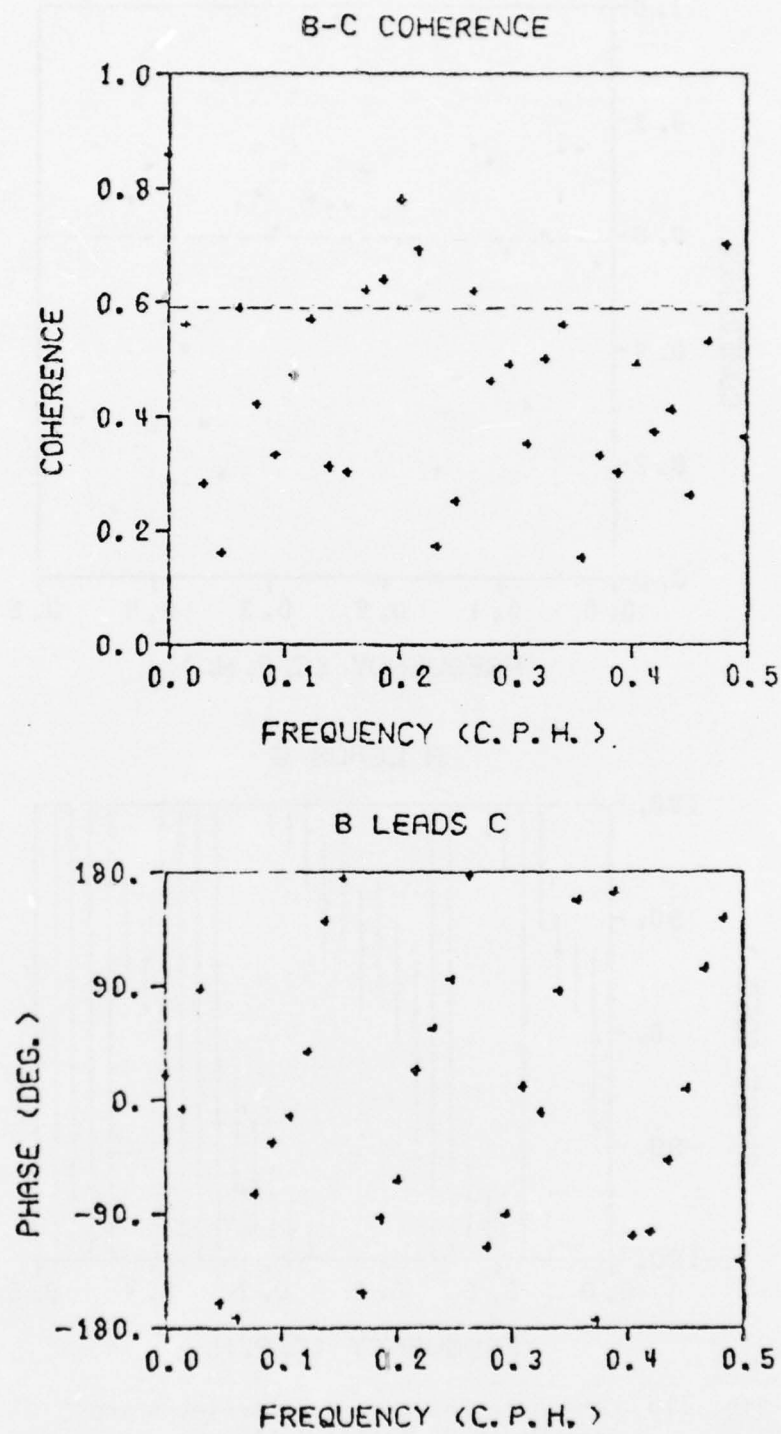


Fig. 11c Coherence between noise series B and C
from March 25 to April 11

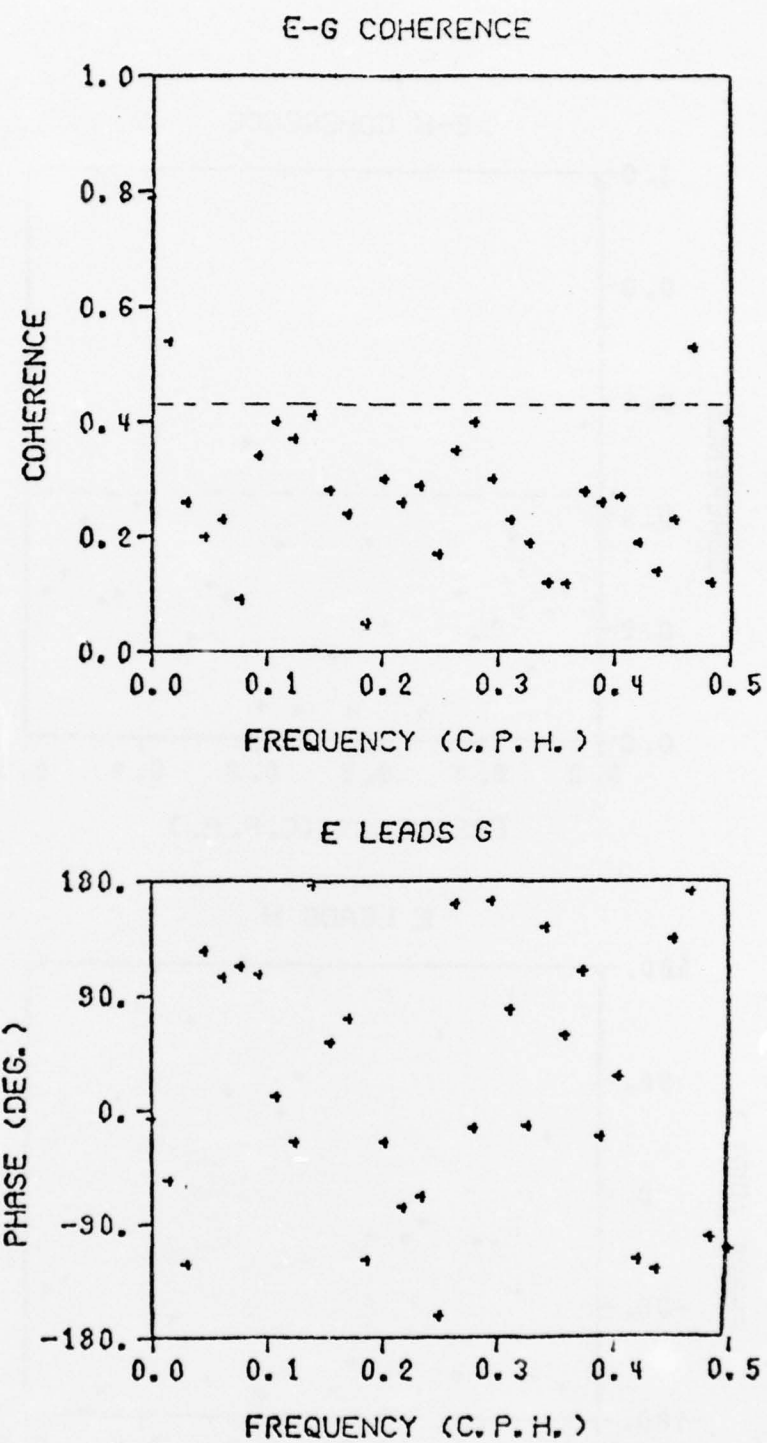


Fig. 11d Coherence between noise series E and G
from May 7 to June 18

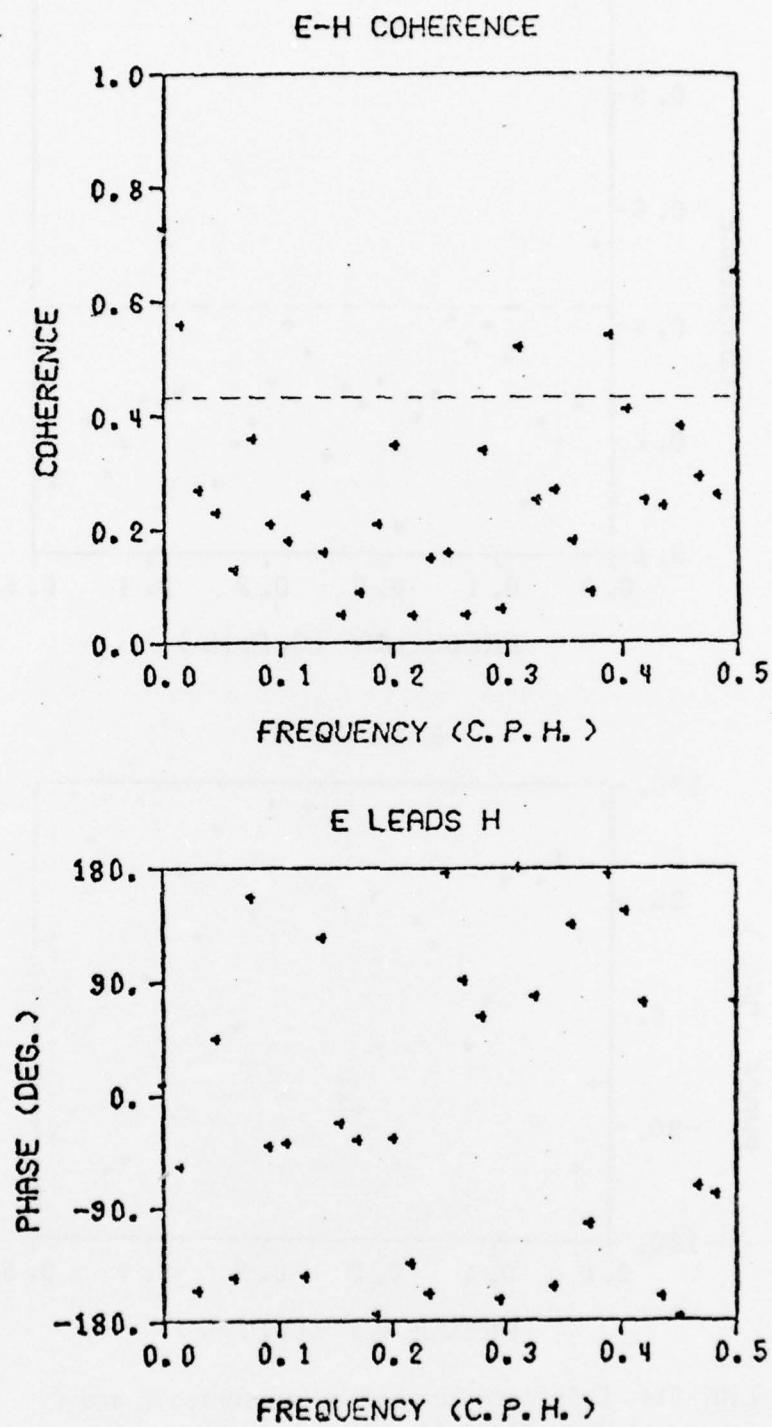


Fig. 11e Coherence between noise series E and H
from May 7 to June 18

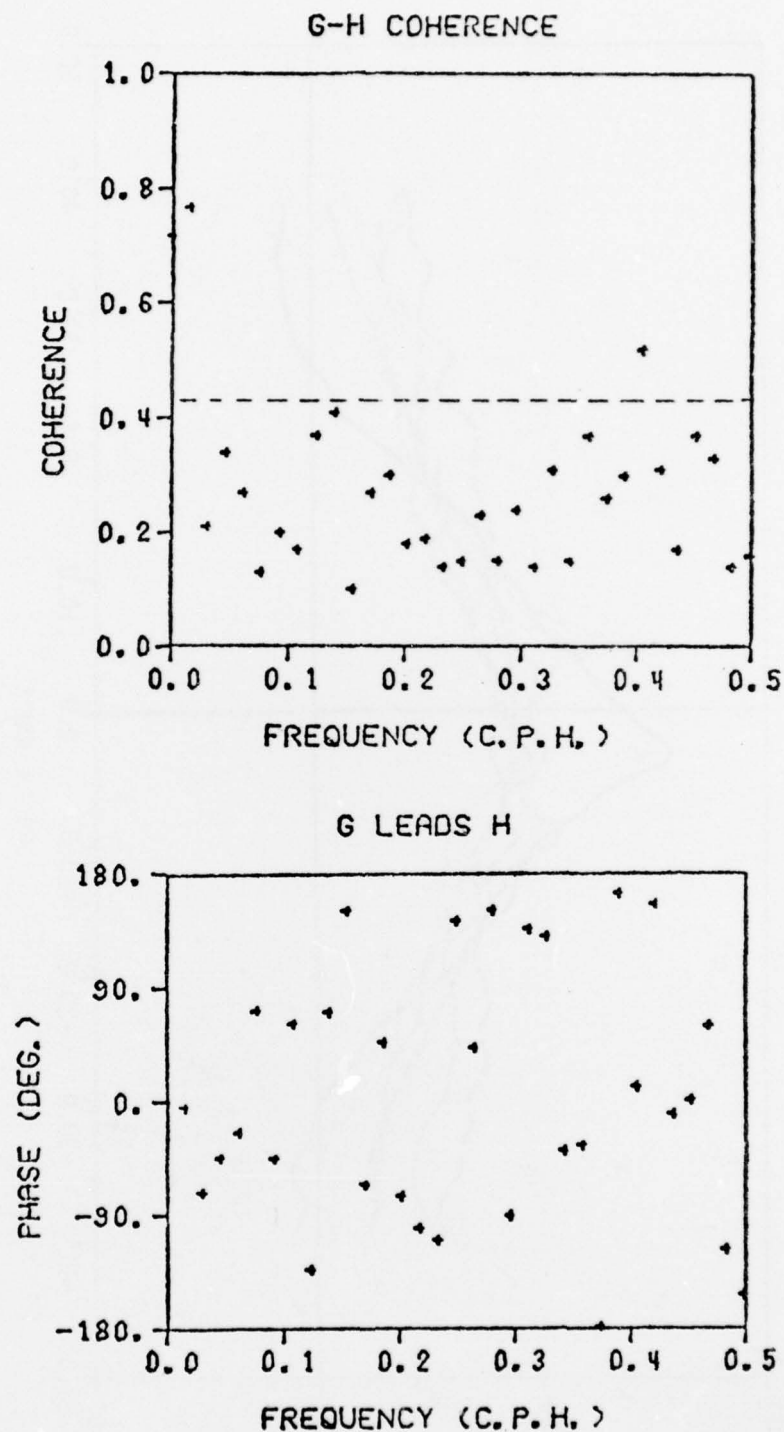
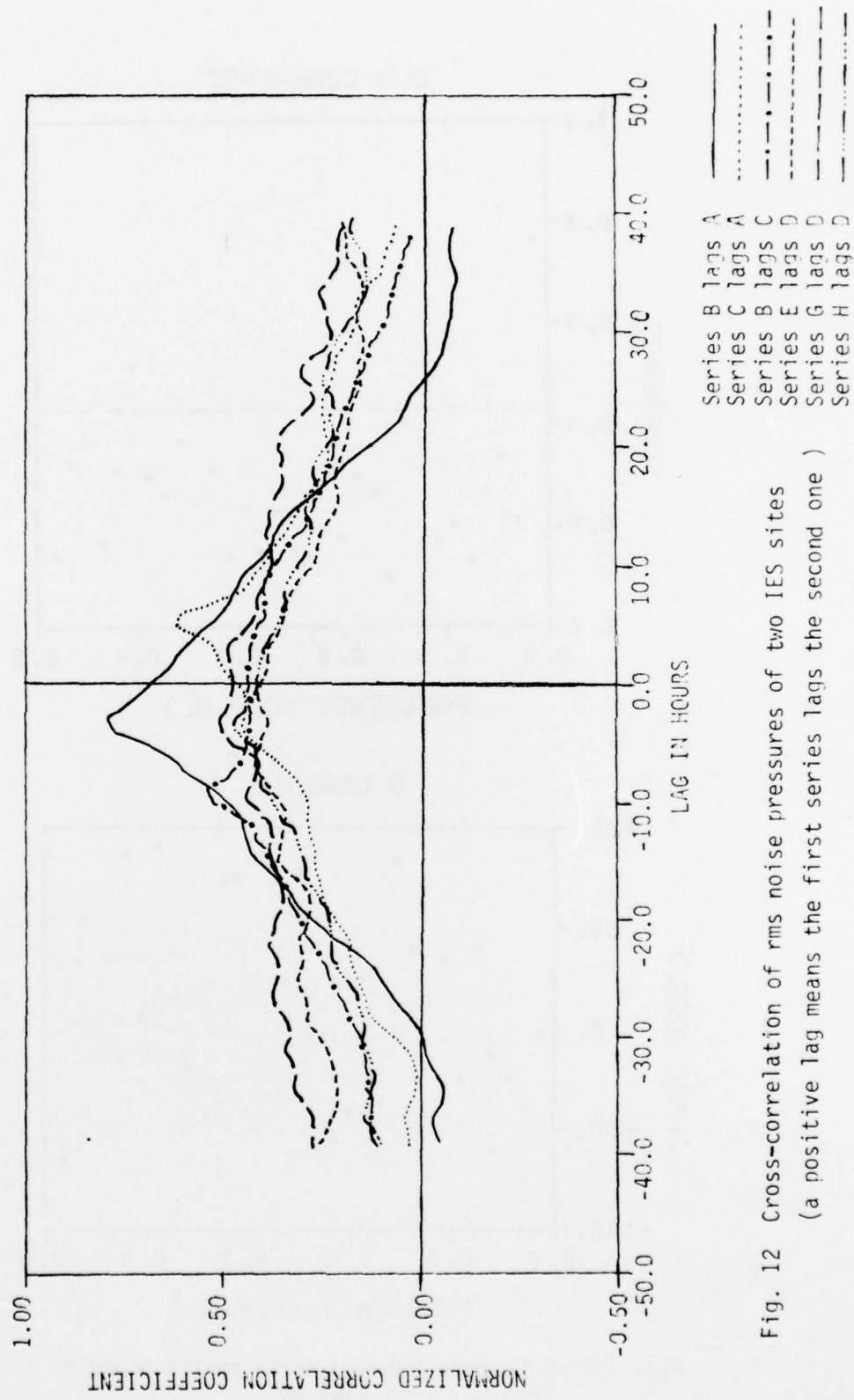


Fig. 11f Coherence between noise series G and H
from May 7 to June 18



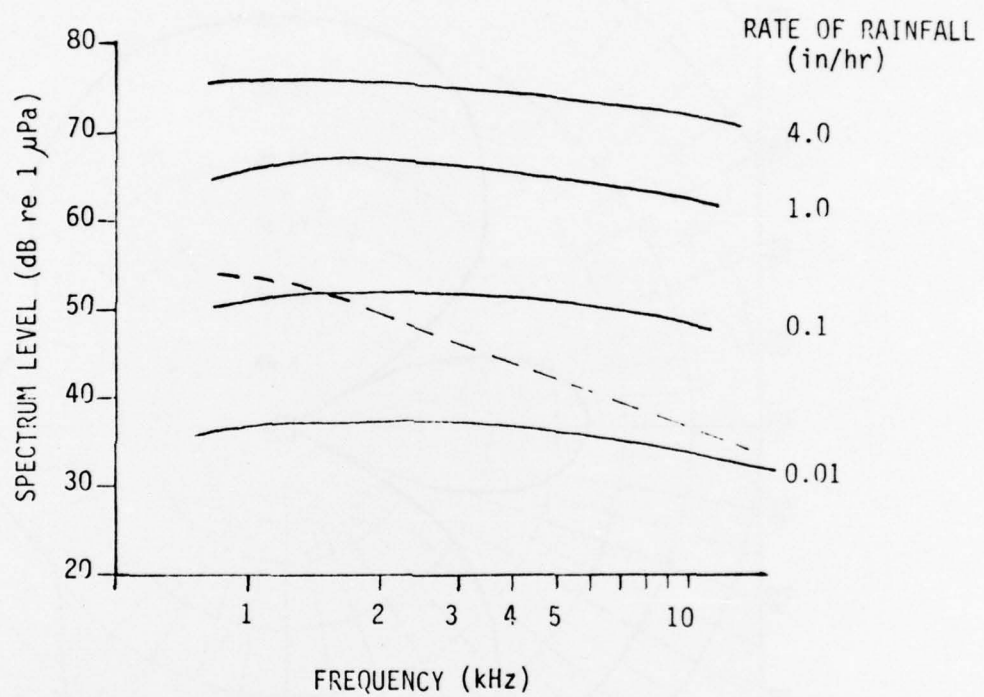


Fig. 13 Theoretical spectra of rain noise for different rates of rainfall. Dashed curve is for deep-sea noise at wind speed 5 knots without rain
(After Franz, 1959)

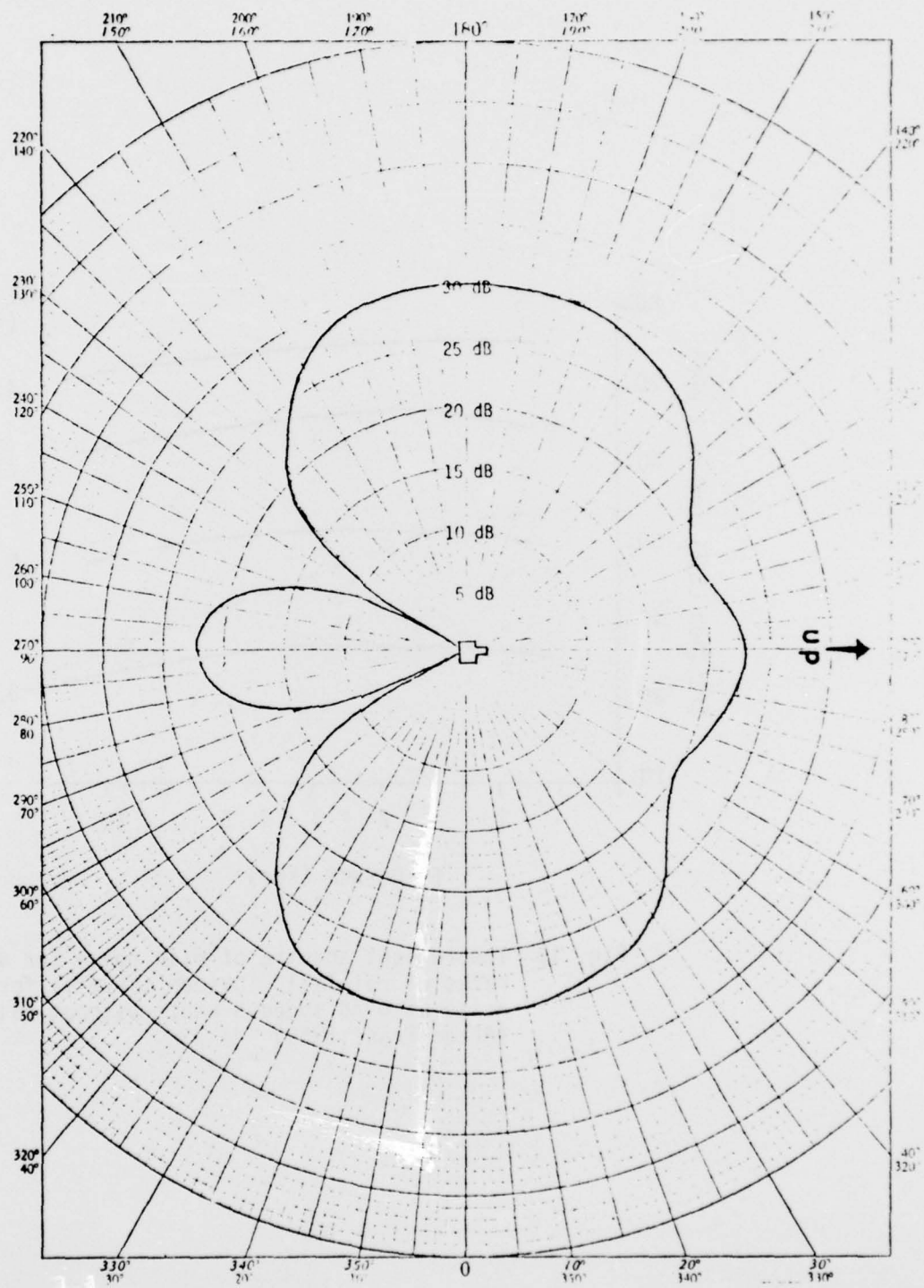


Fig. A1 Directivity pattern of IES receiving hydrophone at 5 kHz

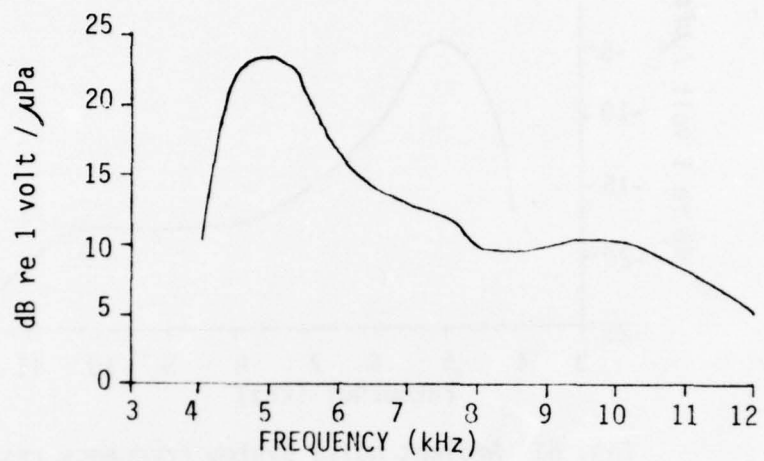


Fig. A2 IES transducer receiving response in horizontal direction

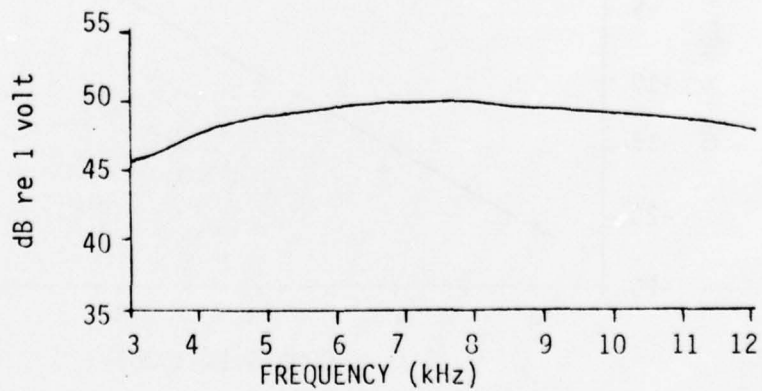


Fig. A3 Frequency response of broad band amplifier

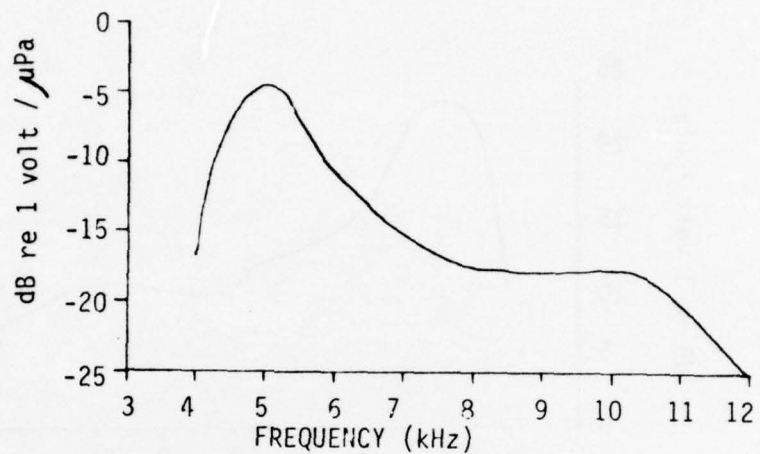


Fig. B1 Ambient noise system frequency response

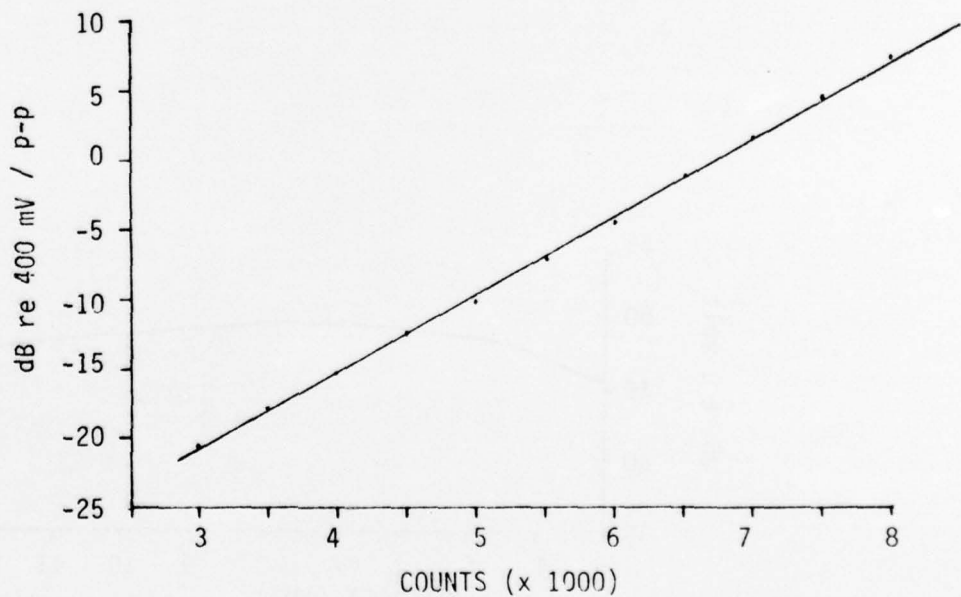


Fig. B2 Input voltage of log detector as a function of output of frequency counter

MANDATORY DISTRIBUTION LIST

FOR UNCLASSIFIED TECHNICAL REPORTS, REPRINTS & FINAL REPORTS
PUBLISHED BY OCEANOGRAPHIC CONTRACTORS
OF THE OCEAN SCIENCE AND TECHNOLOGY DIVISION
OF THE OFFICE OF NAVAL RESEARCH
(REVISED OCT. 1975)

1	Director of Defense Research and Engineering Office of the Secretary of Defense Washington, DC 20301 ATTN: Office Assistant Director (Research)	12	Defense Documentation Center Cameron Station Alexandria, VA 22314
1	Office of Naval Research Arlington, VA 22217 ATTN: (Code 460)	1	Commander Naval Oceanographic Office Washington, DC 20390
1	ATTN: (Code 102-OS)	1	ATTN: Code 1640
6	ATTN: (Code 102IP)	1	ATTN: Code 70
1	ATTN: (Code 200)	3	Ocean Research Office (Code 400) Naval Ocean Research and Development Activity National Space Technology Laboratories Bay St. Louis, MS 39520
1	CRD John Harlett (USN) ONR Representative Woods Hole Oceanographic Inst. Woods Hole, MA 02543		
1	Office of Naval Research Branch Office 495 Summer Street Boston, MA 02210		
6	Director Naval Research Laboratory Washington, DC 20375 ATTN: Library, Code 2620		
1	National Oceanographic Data Center National Oceanic & Atmospheric Administration Rockville, MD 20852		

9 REPORT DOCUMENTATION PAGE		READ INSTRUCTIONS BEFORE COMPLETING FORM
1. REPORT NUMBER URI/GSO Technical Report #77-2	2. GOVT ACCESSION NO. URI/650-Ref-77-2	3. RECIPIENT'S CATALOG NUMBER
4. TITLE (and Subtitle) Oceanic Wind Speed and Wind Stress Estimation from Ambient Noise Measurements	5. TYPE OF REPORT & PERIOD COVERED	
6. PERFORMING ORG. REPORT NUMBER	7. AUTHOR(s) Ping-Tung Shaw, D. Randolph Watts and H. Thomas Rossby	
8. CONTRACT OR GRANT NUMBER(s) N00014-76-C-0236	9. PERFORMING ORGANIZATION NAME AND ADDRESS Ocean Research Office (Code 400) NORDA, Nat'l. Space Tech. Laboratories Bay St. Louis, MS 39520	
10. PROGRAM ELEMENT, PROJECT, TASK AREA & WORK UNIT NUMBERS	11. CONTROLLING OFFICE NAME AND ADDRESS Ocean Research Office (Code 400) NORDA, Nat'l. Space Tech. Laboratories Bay St. Louis, MS 39520	
12. REPORT DATE February 1977	13. NUMBER OF PAGES 76 (2180p)	
14. MONITORING AGENCY NAME & ADDRESS (if different from Controlling Office) NSF	15. SECURITY CLASS. (of this report) Unclassified	
16. DISTRIBUTION STATEMENT (of this Report) Approved for Public Release. Distribution unlimited.	17. DISTRIBUTION STATEMENT (of the abstract entered in Block 20, if different from Report) Approved for Public Release. Distribution unlimited.	
18. SUPPLEMENTARY NOTES		
19. KEY WORDS (Continue on reverse side if necessary and identify by block number) Wind speed Wind Stress Acoustic Ambient Noise Mid-Ocean Dynamics Experiment (MODE-I), it was found		
20. ABSTRACT (Continue on reverse side if necessary and identify by block number) From ship records of wind speed and 5 kHz acoustic ambient noise measured on ocean bottom instruments during MODE-I, we find that the noise records may be used to monitor wind speed and wind stress over the ocean. Time series of wind speeds can be produced from noise measurements via the linear relationship we find between the noise spectrum level and the logarithm of the wind speed. Errors in this conversion are estimated to be less than 5 knots. By independently determining the wind direction, the wind stress has also been (cont on p 1473 B) A		

(in authors)

cont 82 P
1473A)

estimated and vector-averaged.) In this way the mean wind stress is neither fair-weather biased nor systematically underestimated from the mean wind velocity squared. The monthly mean stress from our data is higher than values computed from mean wind speeds or from probability distributions of wind speeds in climatological records. Power spectra of our wind speed records decrease smoothly with increasing frequency ($f=1.5$) for periods between 2 to 50 hours. The noise pressure records exhibited significant coherence between pairs of localities 100 to 200 km apart during the spring, as organized weather fronts passed through the region. Cross-correlation time lags between sites were consistent with a mean propagation of the atmospheric disturbances of 30 km/hr southeastward.